

AD-A138 360

REPETITIVE SWITCHING FOR AN ELECTROMAGNETIC RAIL GUN

1/1

(U) AIR FORCE INST OF TECH WRIGHT-PATTERSON AFB OH

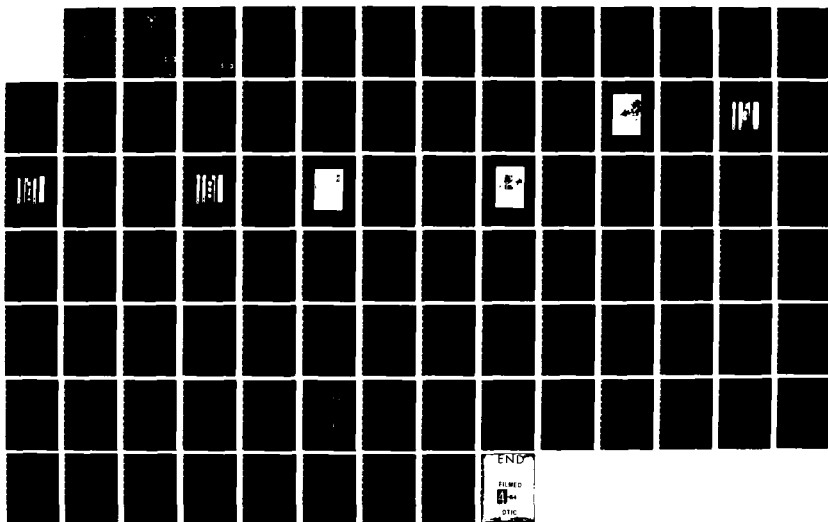
SCHOOL OF ENGINEERING J M GRUDEN DEC 83

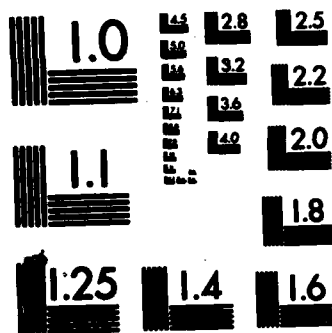
UNCLASSIFIED

AFIT/GE/EE/83D-22

F/G 9/1

NL





MICROCOPY RESOLUTION TEST CHART
NATIONAL BUREAU OF STANDARDS-1963-A

AD A138360.



REPETITIVE SWITCHING
FOR AN
ELECTROMAGNETIC RAIL GUN

THESIS

AFIT/GE/EE/83D-22

James M. Gruden
2nd Lt USAF

DISTRIBUTION STATEMENT A

Approved for public release;
Distribution Unlimited

DTIC
ELECTE
FEB 29 1984

DEPARTMENT OF THE AIR FORCE
AIR UNIVERSITY

AIR FORCE INSTITUTE OF TECHNOLOGY

Wright-Patterson Air Force Base, Ohio

DTIC FILE COPY

84 02 29 046

AFIT/GE/EE/83D-22

REPETITIVE SWITCHING
FOR AN
ELECTROMAGNETIC RAIL GUN

THESIS

AFIT/GE/EE/83D-22

James M. Gruden
2nd Lt USAF

Approved for public release; distribution unlimited.

DTIC
ELECTE
FEB 29 1984
S D
B

REPETITIVE SWITCHING
FOR AN
ELECTROMAGNETIC RAIL GUN

THESIS

Presented to the Faculty of the School of Engineering
of the Air Force Institute of Technology
Air University
in Partial Fulfillment of the
Requirements for the Degree of
Master of Science

by

James M. Gruden
2nd Lt USAF

Graduate Electrical Engineering

December 1983

Approved for public release; distribution unlimited.

Acknowledgements

I would like to thank Major Timothy L. Skvarenina, my thesis advisor, for his guidance and support during this thesis project. Additional thanks go to Captain Gerald D. Clark, Project Engineer in the Aero Propulsion Laboratory, for proposing this thesis topic and for his assistance and guidance during its initial stages. The computer assistance of First Lieutenant Jere L. Brown and First Lieutenant Peter R. Axup is also sincerely appreciated. Finally, a very special thanks to my beautiful fiancée, Marian, for her understanding and patience during the past year.

-James M. Gruden

Accession For	
NTIS GRA&I	<input checked="checked" type="checkbox"/>
DTIC TAB	<input type="checkbox"/>
Unannounced	<input type="checkbox"/>
Justification	
By	
Distribution/	
Availability Codes	
Dist	Avail and/or Special
A-1	

Contents

	Page
Acknowledgements	ii
List of Figures	v
List of Tables	vii
Abstract	viii
I. Background	1
Inductive Energy Storage	1
Opening Switch Considerations	5
Rotary Switch Concept	7
Approach and Presentation	9
II. Rotary Switch	11
Introduction	11
Rotor	11
Brushes	13
Standard Brush	13
Finger (Leaf) Brush	15
Fringe Fiber Brush	17
Drive System	20
Safety Precautions	20
III. Experimental Setup	23
Introduction	23
Power Supply	23
Storage Inductor	25
Load Configuration	25
Instrumentation	27
Experimental Procedure	27
Data Collection	28
IV. Computer Model	30
Introduction	30
Computer Model	30
Computer Program	33
Results	34

V. Results	41
Introduction	41
Results	41
Rotor Comparisons	41
Fringe Fiber Brush Design	49
Finger Brush Design	53
VI. Conclusions and Recommendations	61
Bibliography	65
Appendix A: Computer Program	66
Vita	77

List of Figures

Figure		Page
1.	Basic Inductive Energy Storage Circuit	2
2.	Electromagnetic Rail Gun Circuit	4
3.	Rotary Switch Concept	8
4.	Rotor with Insulating Slot and Top Brushes . . .	12
5.	Standard Brushes and Straps	14
6.	Finger (Leaf) Brushes and Straps	16
7.	Fringe Fiber Brushes and Straps	19
8.	Test Setup with Safety Enclosures and Coil . . .	21
9.	Instrumentation and Power Supply Consoles	24
10.	Cross Section of Stainless Steel Plate Load Configuration	26
11.	Circuit Representing Commutating Phase of the Rotary Switch	31
12.	Switch Current vs. Time as a Function of Switching Frequency	35
13.	Switch Voltage vs. Time as a Function of Switching Frequency	36
14.	Commutation Time vs. Switching Frequency	38
15.	Commutation Time vs. Load Inductance as a Function of Switching Frequency	39
16.	Energy Dissipated in the Switch vs. Load Inductance for an Initial Current of 1 kA	40
17.	Typical Load Current and Voltage Pulses Resulting from the Original Rotor	42
18.	Typical Load Current and Voltage Pulses Resulting from the New Rotor	44

	Page
19. Load Current and Voltage Pulses Resulting from the New Rotor, Fringe Fiber Brushes and a High Inductive Load	52
20. Load Current Waveforms Showing the Effects of Brush Bounce	60
21. Current Flow Through a Standard Brush and Through a New Brush Design During Commutation . .	63

List of Tables

Table	Page
I. Summary of Test Parameters and Results	10
II. New Rotor Switching Data Using Standard Brushes .	46-47
III. New Rotor Switching Data Using Fiber Brushes . .	50-51
IV. New Rotor Switching Data Using Finger Brushes . .	54-55

Abstract

Previous testing on a repetitive opening switch for inductive energy storage has proved the feasibility of the rotary switch concept. The concept consists of a rotating copper disk (rotor) with a pie-shaped insulator section and brushes which slide along each of the rotor surfaces. While on top of the copper surface, the brushes and rotor conduct current allowing the energy storage inductor to charge. When the brushes slide onto the insulator section, the current cannot pass through the rotor and is diverted into the load.

This study investigates two new brush designs and a rotor modification designed to improve the current commutating capabilities of the switch. One brush design (fringe fiber) employs carbon fibers on the leading and trailing edge of the brush to increase the resistive commutating action as the switch opens and closes. The other brush design uses ("fingers") to conduct current to the rotor surface, effectively increasing the number of brush contact points. The rotor modification was the placement of tungsten inserts at the copper-insulator interfaces. It was hoped that the increased resistivity and hardness of the tungsten inserts would reduce the arcing between the brushes and the rotor surface and lessen the arc-related damage of the switch.

The new rotor design was very successful. The arc-related damage at the insulator section interface was reduced by the tungsten inserts and a larger resistive commutating action was observed due to its presence. The fringe fiber brush design did not work well at the high current levels where the switch was designed to operate. In fact, many of the fibers were completely detached from the brush at current levels above 4 kA. The finger brushes also had difficulty conducting current above the 4 kA level. During these runs, the fingers began to melt and, in some cases, the brushes became unsoldered from the brush straps.

Several recommendations for future testing and a new brush design are also presented at the end of the study.

REPETITIVE SWITCHING FOR AN ELECTROMAGNETIC RAIL GUN

I. Background

Inductive Energy Storage

Pulsed power applications require the release of large amounts of energy in very short time periods. Generally, the energy is stored over a "long" time period and then quickly released to the load. The energy can be stored chemically in batteries or inertially in homopolar generators and superflywheels. More importantly, for fast discharge applications, the energy can be stored in the electric field of capacitors or the magnetic field of inductors. Inductive energy storage is of particular interest because its energy storage density can approach 100 times that of capacitive energy storage (Ref 1:314).

Figure 1 shows the basic inductive energy storage circuit. As current from the source (I_0) flows through the inductor and switch S_1 (initially closed), energy is stored in the magnetic field of the inductor. If S_1 opens simultaneously with the closing of S_2 , the inductor will transfer some of its energy to the load. The resistance and inductance of the

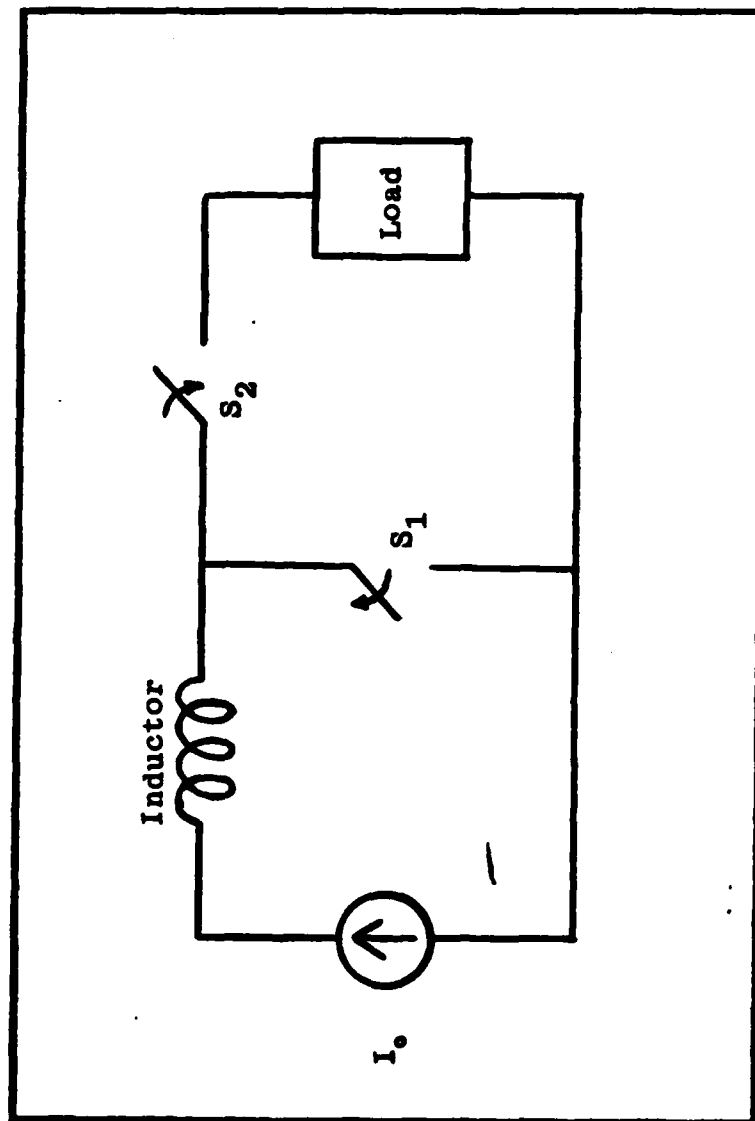


Figure 1. Basic Inductive Energy Storage Circuit

load and switch determine how much of the stored energy is transferred. If the load and switch are purely inductive and resistive respectively, a maximum of 25% of the stored energy can be switched into the load. Maximum energy transfer occurs when the coil and load inductances are equal. In this case, 50% of the stored energy is dissipated in the switch regardless of its design or construction.

Alternatively, if the load is purely resistive, 100% of the stored energy could be transferred, provided both switches are ideal. Clearly, all loads will have some resistance and inductance and caution should be exercised to account for the "stray" inductance and resistance associated with the switch design.

One example of an inductive energy storage system application is the electromagnetic rail gun (Figure 2). The inductor is charged through the closed switch until the required projectile acceleration current (as much as a few MA) is obtained. The switch is then opened and current flows through the upper rail and projectile, returning through the lower rail. The interaction of the magnetic field produced by the rail currents and the current passing through the projectile ($\vec{J} \times \vec{B}$) creates a force (Lorentz) which accelerates the projectile down the rails. When the projectile reaches the muzzle, the switch is closed and the coil is recharged.

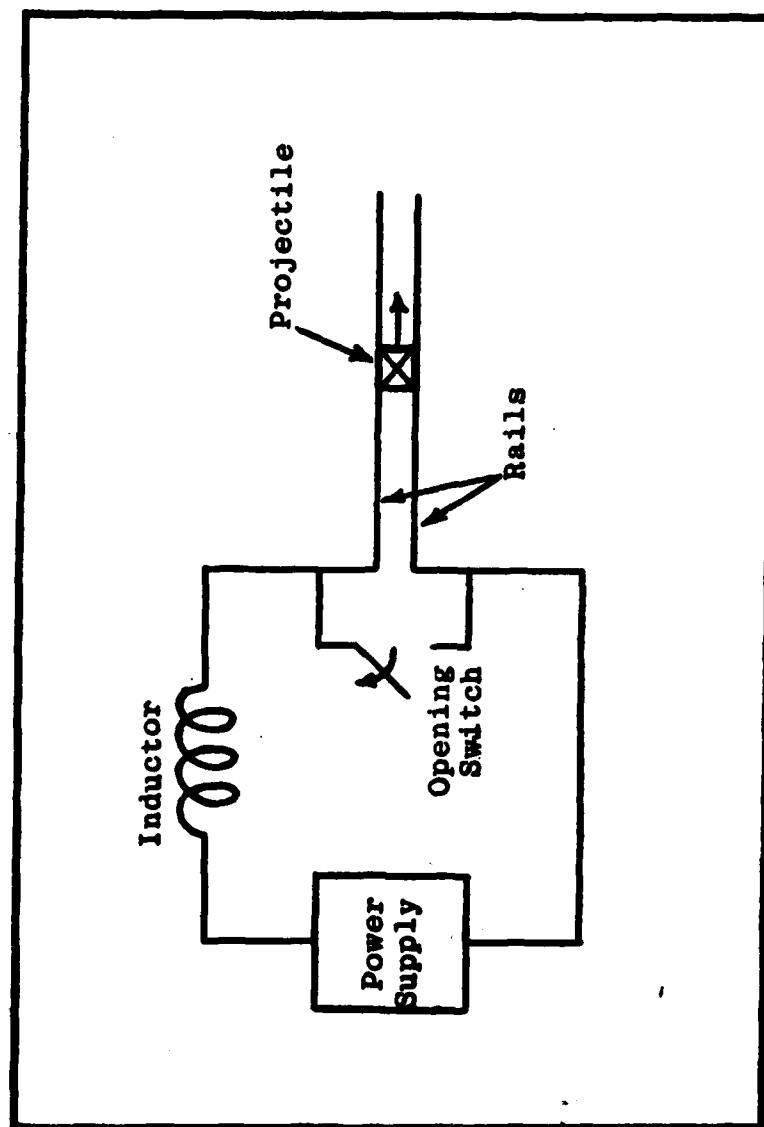


Figure 2. Electromagnetic Rail Gun Circuit

Electromagnetic rail guns can provide higher projectile velocities than conventional chemical propellant guns. This results in increased target damage and decreased time of flight (or increased range). Since velocities can be increased by a factor of four over conventional chemical propellant guns (Ref 2:3), rail guns are the subject of several Department of Defense sponsored research efforts.

Design considerations for inductive energy storage systems include the charging scheme, the inductor and the opening switch. Technical problems are associated with each of these components, but the most difficult problems appear to arise with the repetitive opening switch.

Opening Switch Considerations

The opening switch required for inductive energy storage systems encounters several phases during its operation, each placing performance requirements on the switch. These phases include the conducting, commutating, fully opened and closing phases.

During the conducting phase, the switch must carry high currents (a few hundred kA to a few MA) for long periods of time (typically a 90% duty cycle). This implies that the resistance must be very small to reduce the energy absorbed by the switch. The switch must be capable of dissipating this energy and mechanically surviving the forces associated with the large magnetic fields.

The commutating phase is the most demanding of the four phases. The switch must be capable of developing the commutation voltage (a few kV) in a short time (a few mS). The additional energy transferred during commutation must also be dissipated by the switch.

While the switch is open, the load voltage becomes very high (10 kV - 1 MV). The switch must be able to "standoff" this voltage without breaking down.

The switch closing presents very few problems and is not considered a critical phase of the switching process. However, it should be noted that the inductance present in the switch and load tend to limit how fast the current can be commutated during the closing (and opening) phase.

In addition to the requirements associated with the four switching phases, repetition rates ($10 - 10^5$ Hz) and long lifetimes are desirable opening switch characteristics.

The opening switch design is determined by the criteria previously stated in this section. The necessity of a low resistance, high current switch eliminates gas discharge or plasma switches due to their voltage drop (10's of volts) and high energy loss. Solid state switches have a smaller voltage drop (1-2 V), but the junction area required to handle the large currents would be enormous (Ref 3:5).

The most feasible repetitive opening switch choice appears to be an electromechanical switch employing high

conductivity metals, and metal-to-metal contacts. The switch size would depend on the thermal and mechanical demands of the conducting phase.

Rotary Switch Concept

The rotary switch concept shown in Figure 3 is electromechanical in nature. As the conducting disk rotates, the brushes slide along the disk surface, shunting current from the load. When the high impedance insulating slot passes under the brushes, the area allowing current to flow into the rotor is reduced. A larger resistance results, restricting current and forcing the remaining current toward the trailing edge of the brush. This process continues until the entire brush surface slides onto the insulating slot. When the trailing edge of the brush slides onto the slot, some current continues to flow due to the inductance of the circuit. This results in an arc between the trailing edge of the brush and the conducting disk. As the distance between the trailing edge of the brush and the conducting disk increases, the arc channel stretches, increasing its resistance and decreasing the arc current. Once the current is sufficiently small such that the arc can no longer be sustained, the arc terminates, and the current is completely commutated into the load.

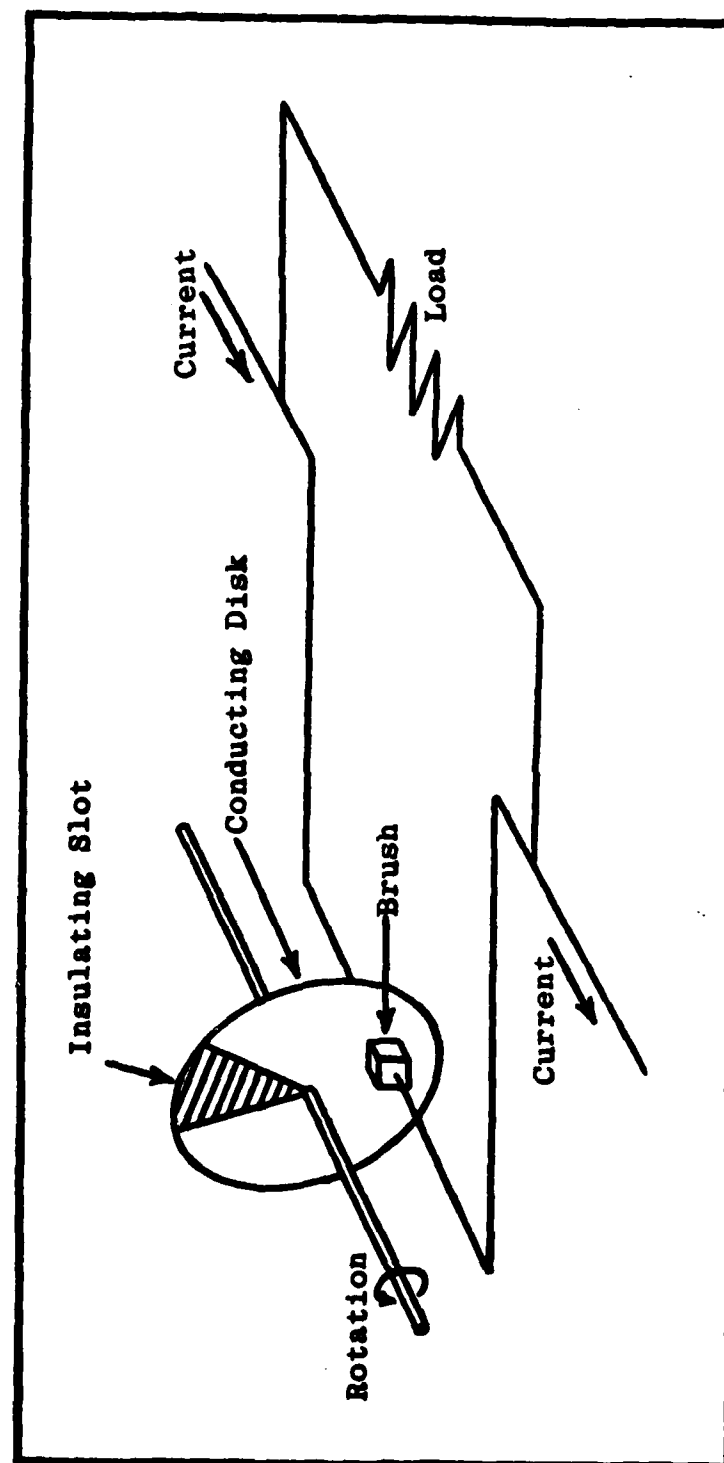


Figure 3. Rotary Switch Concept

A switch based on this concept was built by IAP Research for the Air Force Aero Propulsion Laboratory and has been successfully tested over a wide range of operating conditions. The results of these tests are listed in Table I (Ref 4).

Approach and Presentation

This thesis continued where previous testing on the rotary switch ended. A new rotor and two new brush designs were investigated to determine if the commutation process could be improved and the rotor wear and arcing reduced. Each of the new components was tested while varying the switching frequency, current level, number of brushes, brush pressure and load configuration.

Chapter II contains a detailed description of the rotary switch and each of its components. Particular attention is devoted to the new brush designs and their potential for improved operation. This is followed by a description of the experimental setup in Chapter III. The description starts with the power supply and includes the storage inductor, switch, load, instrumentation and data collection process. In Chapter IV, a computer model is presented which attempts to simulate the opening switch process. Finally, Chapter V presents the test results while Chapter VI contains the conclusions and recommendations for future testing of the rotary switch.

Table I**Summary of Test Parameters and Results**

Total Commutations	>5,000
Frequency	0.9 - 61 Hz
Current	0.3 - 11.0 kA
Current Density	0 - 2.2 kA/cm²
Contact Voltage Drop	0.2 - 1.1 V
Maximum Energy Per Pulse	6.2 kJ
Maximum Pulse Power to Load	653 kW
Maximum Avg. Power to Load	65.3 kW
Test Duration	0 - 3.9 Sec
Maximum Commutation Voltage	62.4 V
Static Voltage Standoff	1.0 kV
Load Resistance	1.5 - 6.0 mΩ
Load Inductance	5 nH
Pulse Width	1.7 - 80 mSec
Opening Speed	0.8 - 61 m/Sec
Contact Force	40 - 290 N

II. Rotary Switch

Introduction

In this chapter, the new rotor and brush designs are described in detail. The drive system for rotating the switch and safety precautions are also discussed.

Rotor

The new rotor shown in Figure 4 was built by the 4950th Test Wing Fabrication/Modification and Support Division at Wright-Patterson Air Force Base. The copper disk is 1.43 cm thick with a 38 cm diameter. The disk is held on a vertical shaft by two aluminum hubs. The two holes located in the top aluminum hub opposite the insulating slot provide the balancing required for high rotating speeds (up to 4,000 RPM).

The pie-shaped insulating slot is made of Hysol R9-2039 epoxy resin. This resin was selected for its bonding compatibility with copper (Ref 5:5). The epoxy resin stops just beyond the inside brush track and extends .05 cm into the rotor surface. The insulating slot represents 10% of the switching cycle, resulting in a .9 duty cycle.



Figure 4. Rotor with Insulating Slot and Top Brushes

Tungsten inserts 0.5 cm wide (0.5% of the switching cycle) were machined into the rotor surface at the two epoxy-copper boundaries. It was hoped that two benefits would be obtained by using the tungsten inserts. First, since tungsten is a much harder material than copper, the rotor wear during the commutation should be reduced. Secondly, the higher resistivity should reduce the arc current available during the opening of the switch.

Brushes

Three types of brush designs were investigated during the switch testing. The designs included the standard, finger and fringe fiber brushes.

Standard Brush. The standard brush was a 1 cm³ block of CM1S copper graphite made by Morganite Inc., South Carolina. The brushes were torch soldered to zirconium-copper straps, 0.0762 cm thick, 0.9271 cm wide and 9.525 cm long (Figure 5).

The brush strap mounts were capable of holding five brushes on the top side of the rotor as well as on the under side. Figure 4 shows three brush straps in place with an available slot on either side.

The brushes made contact with the rotor surface via cantilever action. A pneumatically controlled lexan piston pushed on the brush strap near the brush, forcing the brush

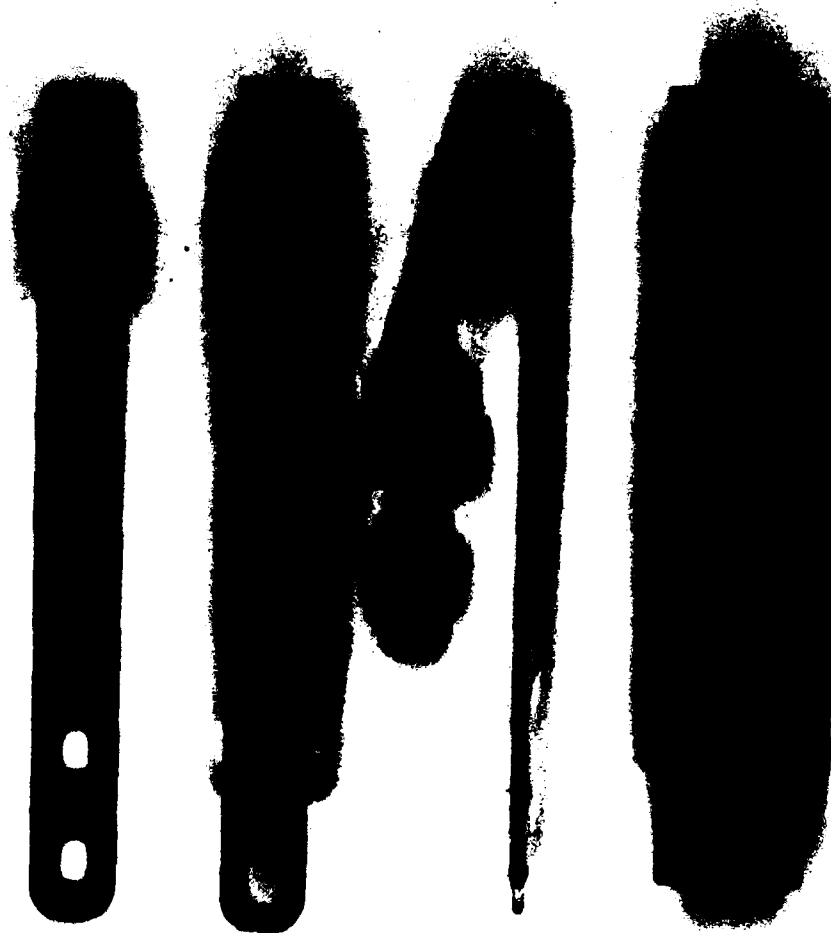


Figure 5. Standard Brushes and Straps

to contact the rotor surface. Each brush could be independently actuated, and the brush contact pressure was controlled by a pressure regulator in the nitrogen gas line. The tension on the brush strap was sufficient to lift the brush from the rotor surface once the air pressure was removed. Enough brush pressure was maintained to provide a low contact voltage drop and to minimize rotor wear. The force on a brush strap ranged from 20 to 34 Nt.

The problem associated with brushes with flat contact surface areas is that there are only several spots which actually conduct the current. During one experiment, it was determined that with a surface contact area of 2 cm^2 , and pressures ranging from 0.5 - 1.1 kg, the number of actual contact spots varied from 6 to 18. This is the equivalent of reducing the contact area by more than three orders of magnitude (Ref 6:365)!

Finger (Leaf) Brush. The second type of brush had little metal "fingers" extending from the brush strap and contacting the rotor surface (Figure 6). Since each finger should conduct current, the number of contact points can approach the number of fingers contacting the rotor surface. The increase in the brush contact area should improve the current carrying capability of the brush.

Two sets of finger brushes were fabricated by the lab technicians in the Aero Propulsion Laboratory at Wright-



Figure 6. Finger (Leaf) Brushes and Straps

Patterson AFB. The brushes were constructed by cutting .0457 cm slots into thin cadmium-copper sections 1 cm wide and placing cadmium-copper spacers between each section. Next, a wire was laced through the sections and spacers to keep them aligned. Finally, the brushes were silver soldered to the brush straps.

The first set had six fingers in a row, ten rows of fingers, and .038 cm spacers, while the second set had six fingers in a row, eight rows of fingers, and .0635 cm spacers.

Cadmium-copper was selected for the brush material due to its reluctance to sustain an arc (Ref 6:334) and its availability. (Zinc-copper and bismuth-copper are other alloys which reduce arcing, but they are more difficult to obtain.) Cadmium-copper also retains its high tensile strength and good electrical conductivity at temperatures considerably higher than the softening point of copper (about 200°C).

Fringe Fiber Brush. During the 1960's, a multi-element contact brush using carbon fibers was developed in Great Britain. Tests on a dummy commutator rig showed the brush benefited from a large number of contact points while its strength and flexibility enabled it to follow surface irregularities. Its contact resistance was found to vary more nearly in inverse proportion to the area of the brush covered by the

commutator segment than that of the solid conventional brush. Since the current commutation process was due to an increased resistance, arcing would not occur under conditions where conventional brushes would arc.

Unfortunately, a major disadvantage was discovered -- the material had a very high coefficient of friction, even at low pressures. This produced unacceptable commutator wear and a much larger contact voltage drop than conventional brushes due to deposits of very dark cuprous oxide.

In 1971, a patent was filed for the fringe fiber brush design (Ref 7:85). The design consisted of a conventional monolithic (solid) brush with carbon fibers attached to the trailing edge. This combined the characteristics of the conventional brush with the additional commutating advantages provided by the carbon fibers.

The Morganite brush design for this thesis was very similar to the fringe fiber brush. In addition to carbon fibers on the trailing edge of the brush, carbon fibers were also placed on the leading edge (Figure 7). This would hopefully reduce any possible arcing on both the leading and trailing edge of the brush.

The large currents carried by the brush straps resulted in heating of the brush strap-brush solder connection. At times, the temperature was sufficient to soften the solder.



Figure 7. Fringe Fiber Brushes and Straps

To avoid separation of the brush from the brush strap, a set screw was inserted through the brush strap and into the brush (Figure 7).

Drive System

The rotor was driven via a Reliance Electric A-CV*S Drive Controller. The controller regulated a 10 horsepower AC motor which was directly connected to the rotor shaft. A potentiometer on the remote Operator's Control Station (left center of Figure 9) allowed the user to set the rotor speed. A start/stop rocker switch let the rotor speed ramp up to its preset value or ramp down until it stopped. The output frequency from the Drive Controller ranged from approximately 5 to 60 Hz.

Safety Precautions

Due to the potential hazards while running the switch, several safety precautions were exercised during test runs.

To contain any high velocity fragments from rotor or brush assembly disintegration, a containment vessel was placed around the rotor as shown in Figure 8. The vessel had a 2.38 cm thick lexan top which allowed for viewing during switch operation.

Metal panels were installed around the drive system (motor, shaft and couplings) to eliminate potentially severe

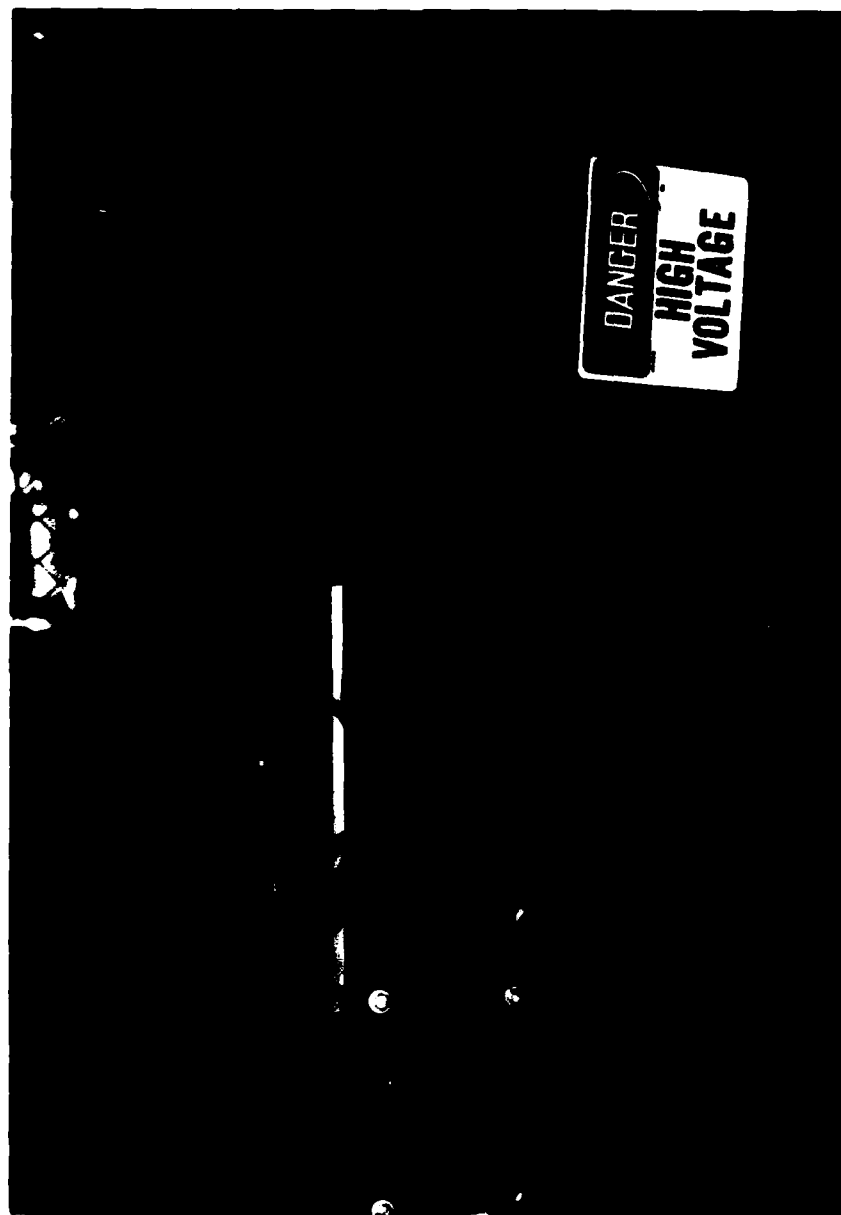


Figure 8. Test Setup with Safety Enclosures and Coil

hazards to operators resulting from drive system malfunctions (Figure 8).

In addition to the enclosures, four flashing lights, a "DANGER HIGH VOLTAGE" sign and a yellow rope around the switch area warned any bystanders of the potential hazards of the area.

III. Experimental Setup

Introduction

This chapter describes the components of the inductive energy storage circuit which were used during the switch tests as well as the instrumentation which monitored the current and voltage signals.

Power Supply

The power supply for the switch tests was a 5 MW supply made by Ling Electronics. It contained a three phase, full wave bridge rectifier capable of providing 12,500 amps at 400 volts. The SCR bridge and associated control circuitry were located in an outdoor metal-clad shelter. The remote control panel for the supply was located near the rotary switch test setup and is pictured on the right side of Figure 9.

The power supply was the limiting factor during the test runs, providing a maximum current of approximately 7.52 kA. At least fifteen SCR fuses were blown while running the supply at higher current settings and the large ripple at low current settings made it difficult to obtain accurate



Figure 9. Instrumentation and Power Supply Consoles

readings. During one run, the supply chose to ramp to infinity and blew several fuses in the shut down process.

Storage Inductor

The energy storage inductor was fabricated by the 4950th Test Wing Fabrication/Modification and Support Division located at Wright-Patterson AFB. The coil was a single layer solenoid 0.8 m long and 0.4 m in diameter. Its winding had 56 turns of 1.27 cm square copper bar. The computed inductance and resistance were 500 μH and 7.85 $\text{m}\Omega$ respectively. The calculated time constant was 63.7 mS . The coil is pictured on the right side of Figure 8.

Load Configuration

The load was a series of ten 20 cm by 28 cm stainless steel plates .16 cm thick separated by mylar sheets. Slots were cut into alternating ends of the mylar sheets. Silver-plated multilam was then placed into the slots to allow current to flow down one stainless steel plate, up the next plate and so forth (Figure 10). This particular load configuration had a resistance of 6.0 $\text{m}\Omega$ (Ref 4).

As testing progressed, inductance was added to the load to increase the load voltage. This was accomplished by sliding the stainless steel plates further out on the buss bars and by introducing a three-turn loop (38 cm diameter) into the load circuit.

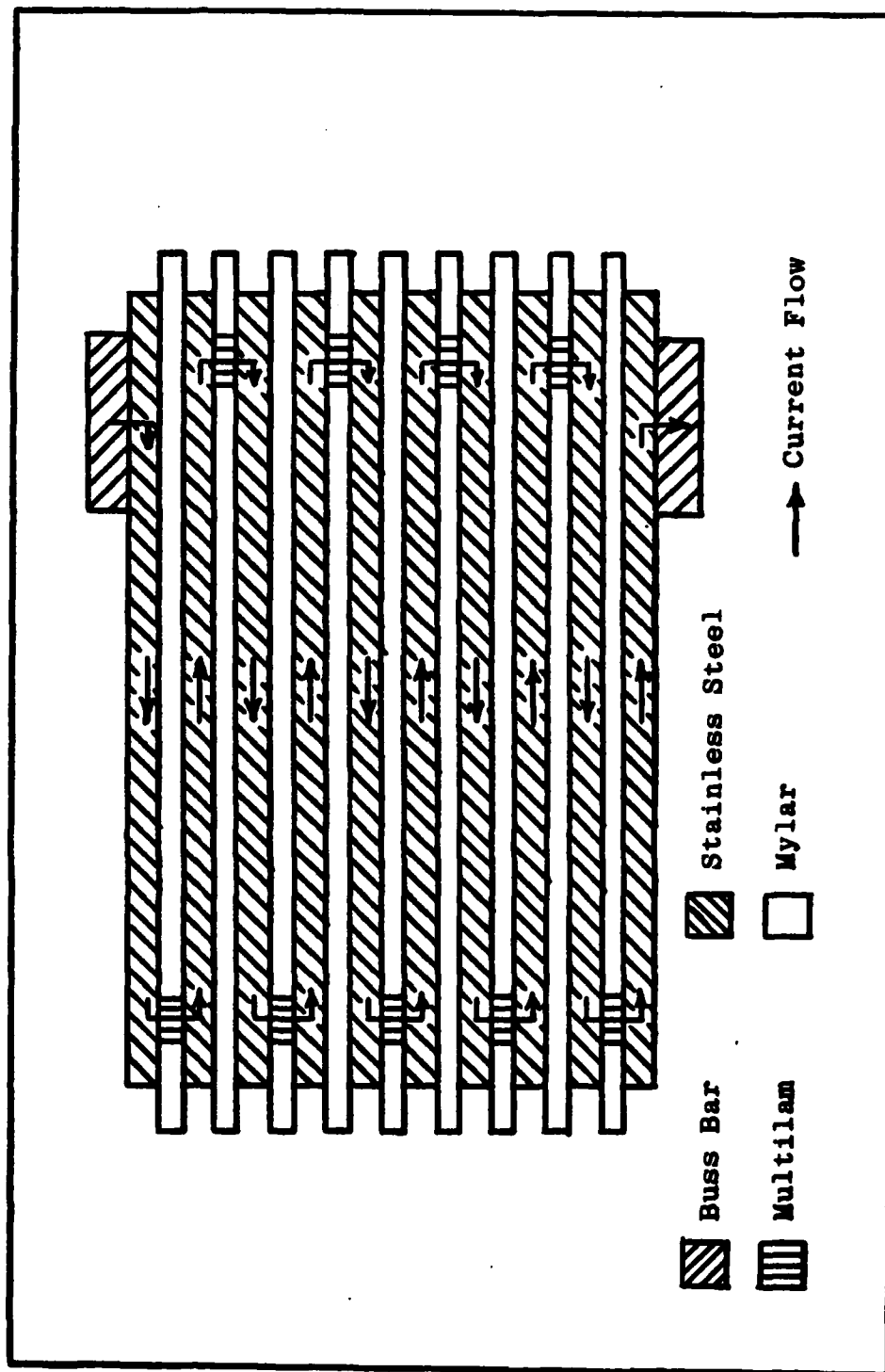


Figure 10. Cross Section of Stainless Steel Plate Load Configuration

Instrumentation

Three currents were monitored during each test -- the power supply, switch and load currents. Each current was sensed using a Rogowski coil. The Rogowski coil output was integrated and then sent via a patchbox to a Honeywell CRT Visicorder model 1858 (left side of Figure 9). The switch and load voltages were also recorded by the visicorder. The visicorder oscillographs were then used to obtain the experimental data.

Experimental Procedure

Once the power supply current, rotor speed and brush pressure were set and the previously mentioned safety precautions enforced, the testing procedure was as follows.

The rotor speed was allowed to ramp up to the value set on the remote Operator's Control without the brushes being activated or the power supply being turned on. Just before the power supply was turned on, the visicorder, integrators and brush pressure were all activated by a single switch. As the power supply current ramped up to its preset value, the visicorder traced the integrated outputs of the Rogowski coils and the switch and load voltages. A typical test ran for 3-5 seconds, enough time to obtain several switching pulses at the desired current level. Once the switching data was obtained, the power supply was shut down and the

visicorder, integrators and brush pressure were all turned off.

Data Collection

As previously mentioned, the visicorder oscillographs were used to record the switch voltages and currents. Obtaining exact values from the oscillographs was limited for several reasons.

The power supply introduced ripple variations in all of the current readings. At the lower current settings, the supply operated as if all the phases of the rectifier circuit were not working. At higher current settings, all the phases appeared to be working and the ripple was significantly reduced. Due to the influence of the ripple, average current values were selected which may deviate slightly from the actual average reading.

The voltage readings were also affected by the power supply. While the switch was closed, the switch voltage was very small, often less than a volt. For that reason, the most sensitive trace setting was chosen. While sensing the small switch voltages, power supply variations and noise associated with the power supply and drive system were also recorded. Once again, average values were chosen which may deviate from the actual average reading.

Finally, the integrators tended to drift at times for no apparent reason. Since both the load and switch currents returned to zero during the switching cycle, a new zero level for each current was established on the oscillograph. However, the power supply current did not return to zero during a run and any associated drift could not be detected.

IV. Computer Model

Introduction

A computer program written in Fortran Version 5 was developed in an attempt to model the commutating phase of the rotary switch. The chapter begins with a description of the computer model, follows with an explanation of the computer program and concludes with the results of the program. A listing of the computer program and a sample output can be found in Appendix A.

Computer Model

A circuit analysis approach was chosen for the computer model and Figure 11 shows the circuit which was modeled. Using the two loop currents I_1 and I_2 , two differential equations were written and solved using the finite difference method (Ref 8:A-27).

Since current from the energy storage coil can be considered a constant during the brief commutating phase, the coil inductance was given an initial current value equal to the current which was to be switched into the load.

The varying switch resistance as the brushes slide from the copper surface of the rotor onto the epoxy insert was

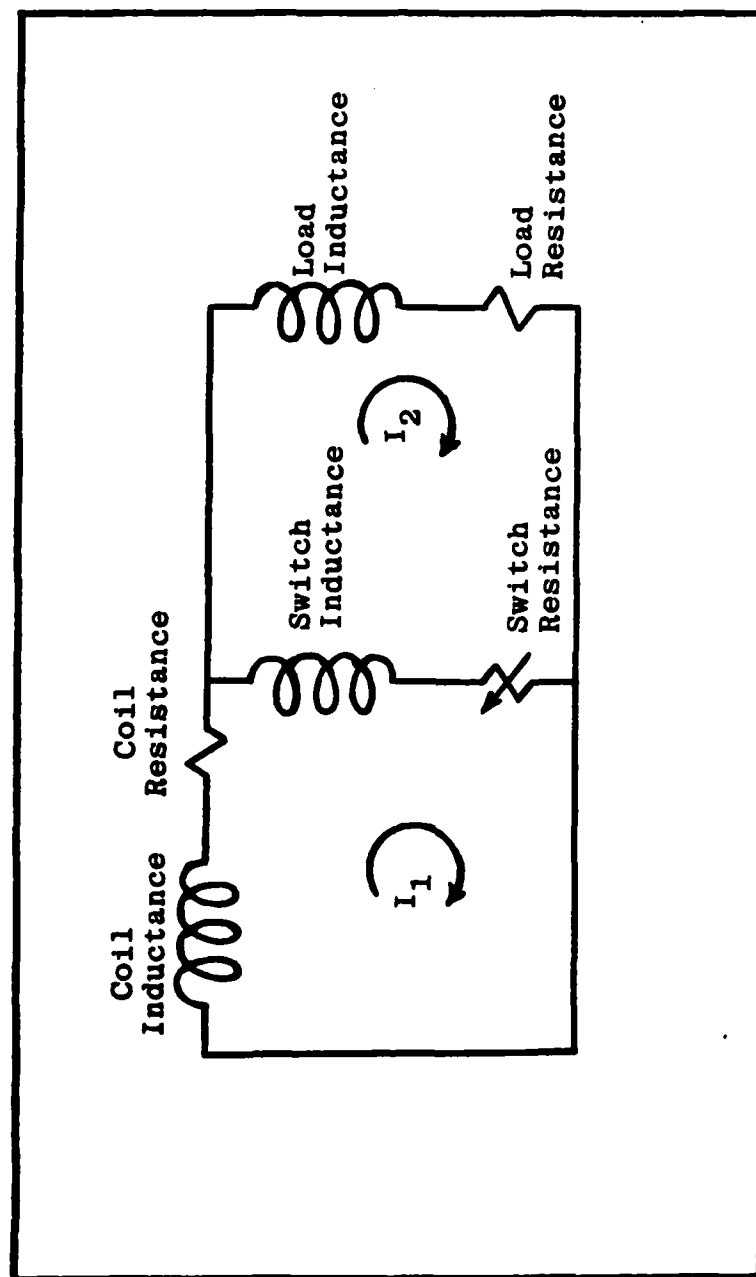


Figure 11. Circuit Representing Commutating Phase of the Rotary Switch

modeled as a linearly increasing resistance starting at 0Ω at time equal to zero and ramping up to $100\text{ M}\Omega$ at time equal to 1% of the switching cycle. (This was the approximate time calculated for the brushes to slide completely onto the epoxy insert.)

The component values used in the computer program were chosen either from laboratory measurements or from component design specifications. The parameters which varied during the switch tests (current level, switching frequency and load inductance) were values which the user could enter directly from the terminal.

The computer model worked well with a time step of 10^{-12} seconds. Since an output tabulation for each iteration would be excessively long, an output interval value was also entered from the terminal. This value determined how many iterations would occur before the tabulated output values were printed.

The computer model does not take into account physical phenomena such as arcing and brush bounce due to surface irregularities at the epoxy-copper boundary. Therefore, the values of switch voltage and commutation rate which this model computes are not consistent with the actual values obtained during the switch tests. However, the model does accurately show the relationship between the switch test

parameters (current level, rotor speed and load configuration) and other important switching characteristics such as commutation rate and switch energy dissipation.

The plots generated from the computer model were obtained using the DISSPLA plotting routine available on Tektronics terminals.

Computer Program

The computer program begins by declaring the variables and arrays used in the program. Next, circuit components whose values remain constant for the duration of the computer run are established. The current level, switching frequency, load inductance and output interval are then entered from the terminal. This is followed by specifying the time step and the initial conditions.

Once the initial conditions are entered into the array locations (for plotting purposes), the finite difference method for solving differential equals is initiated. This method calculates a differential value of I_1, I_2 and switch resistance, and then uses these values to solve for I_1, I_2 and the switch resistance for a particular iteration. The program loops through the finite difference method incrementing time for each successive loop until the current through the switch equals .1% of its original value. Each time an output interval occurs, the program tabulates switch

resistance, switch current, load current, switch voltage and energy dissipated in the switch as functions of time.

If the output interval chosen is too small, the arrays storing values for the plotting routine will not be able to hold all of the values (limited to 60 points). On the other hand, if it is chosen too large, the plots will not be smooth. For these reasons, the number of points in each array is printed out, enabling the user to determine the optimum output interval.

The final section of the program calls the DISSPLA plotting routine. Three curves are plotted on each of two graphs. The two graphs plot switch current and switch voltage versus time as a function of switching frequency.

Results

Figure 12 shows how the current through the switch decreases as a function of time once the switch begins to open. The load in this case has a resistance of $27\text{ m}\Omega$ and an inductance of $.7\text{ }\mu\text{H}$, while the switch inductance equals $.7\text{ }\mu\text{H}$. Curves for three switching frequencies (10 Hz, 50 Hz and 100 Hz) are plotted. The switch voltages associated with each of the currents are shown in Figure 13. As expected, a higher switching frequency reduces the commutation time and increases the voltage across the inductive component of the load.

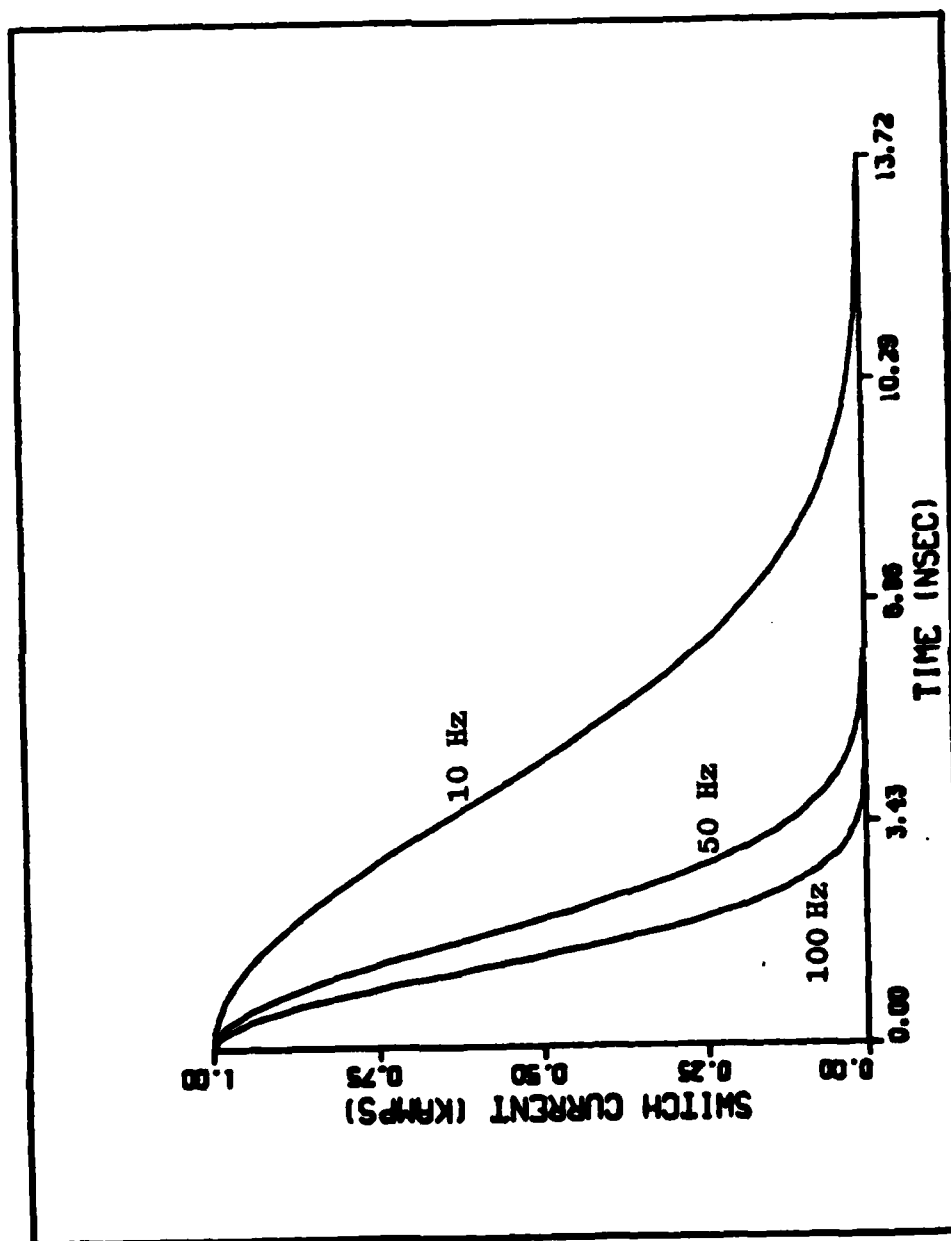


Figure 12. Switch Current vs. Time as a Function of Switching Frequency

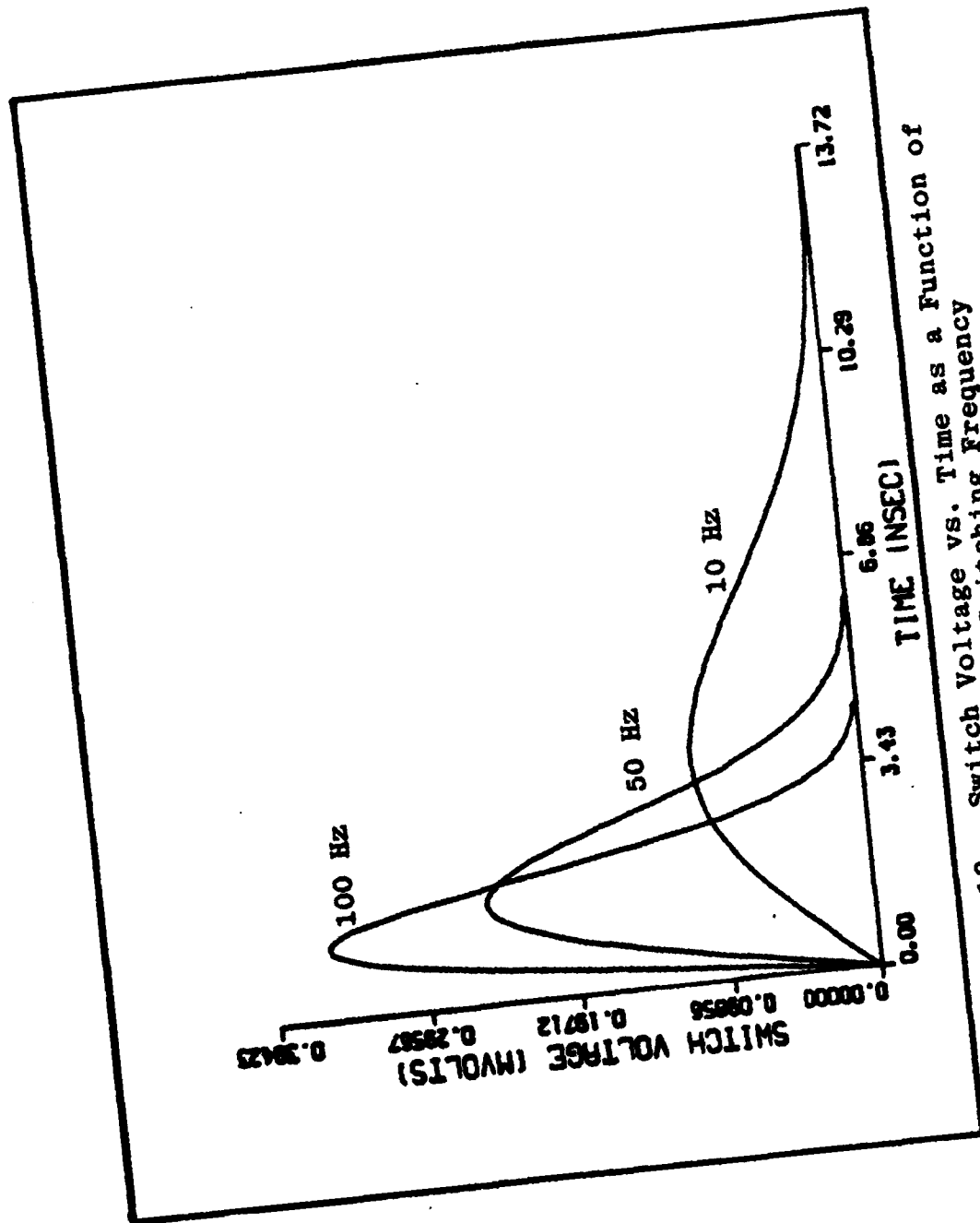


Figure 13. Switch Voltage vs. Time as a Function of Switching Frequency

For the next two plots, the commutation time is defined as that instant in time when the switch current decreases to 10% of its initial value.

Figure 14 shows the commutation time as a function of the switching frequency for a load of $27\text{ m}\Omega$ and $.7\text{ }\mu\text{H}$. It can be seen that a minimum commutation time of about 3 nS is approached. The combination of the switch inductance ($.7\text{ }\mu\text{H}$) and load inductance is responsible for the minimum commutation time.

Figure 15 shows the commutation time versus the load inductance as a function of the switching frequency. Note that each switching frequency has a minimum commutation time despite reducing the load inductance. In this case, the switch inductance ($.7\text{ }\mu\text{H}$) is primarily responsible for the minimum commutation time.

Finally, Figure 16 plots the energy dissipated in the switch versus the load inductance for an initial current of 1 kA . As expected, a larger load inductance slows down the commutation rate, forcing the switch to absorb more energy. It should be noted that the switch must always dissipate some energy despite reducing the load inductance.

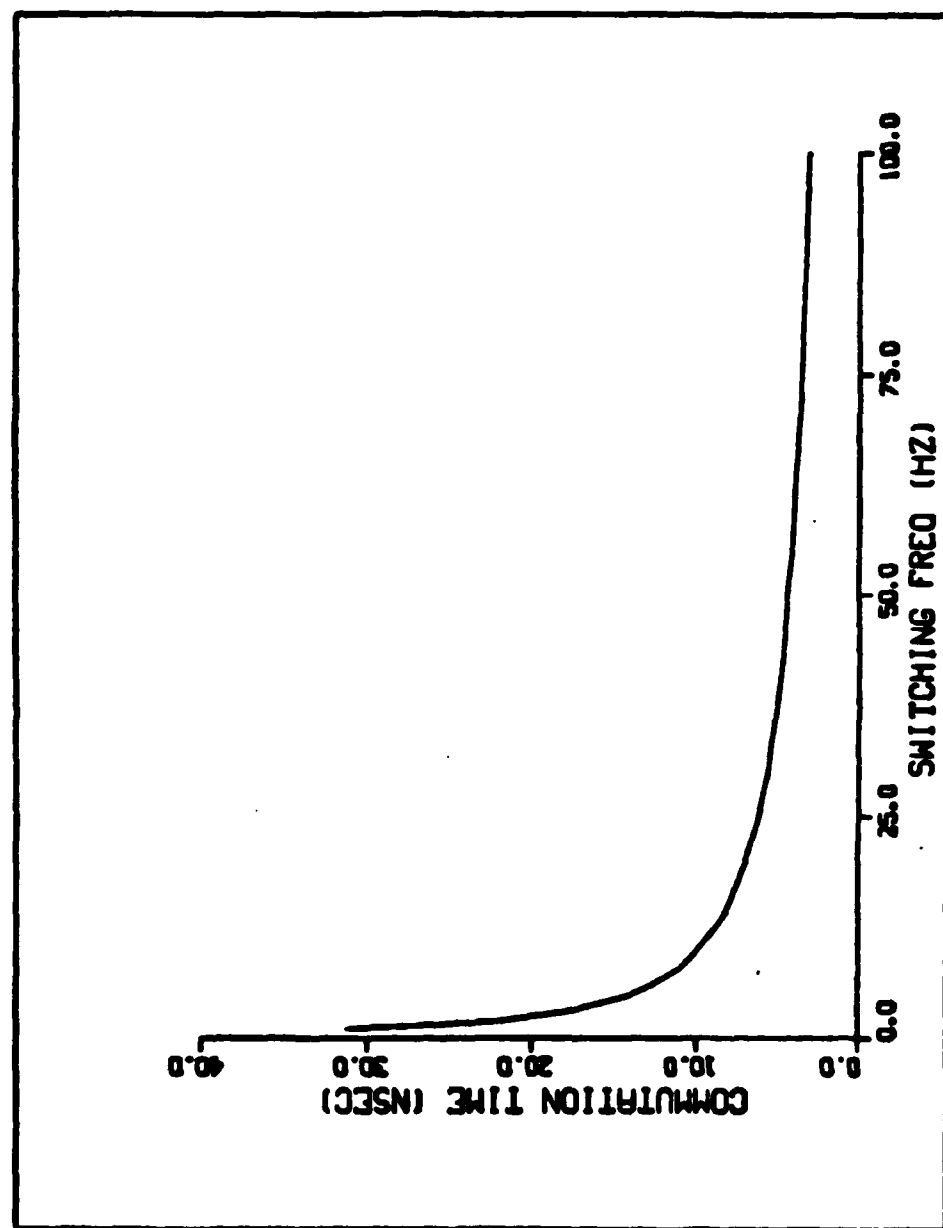


Figure 14. Commutation Time vs. Switching Frequency

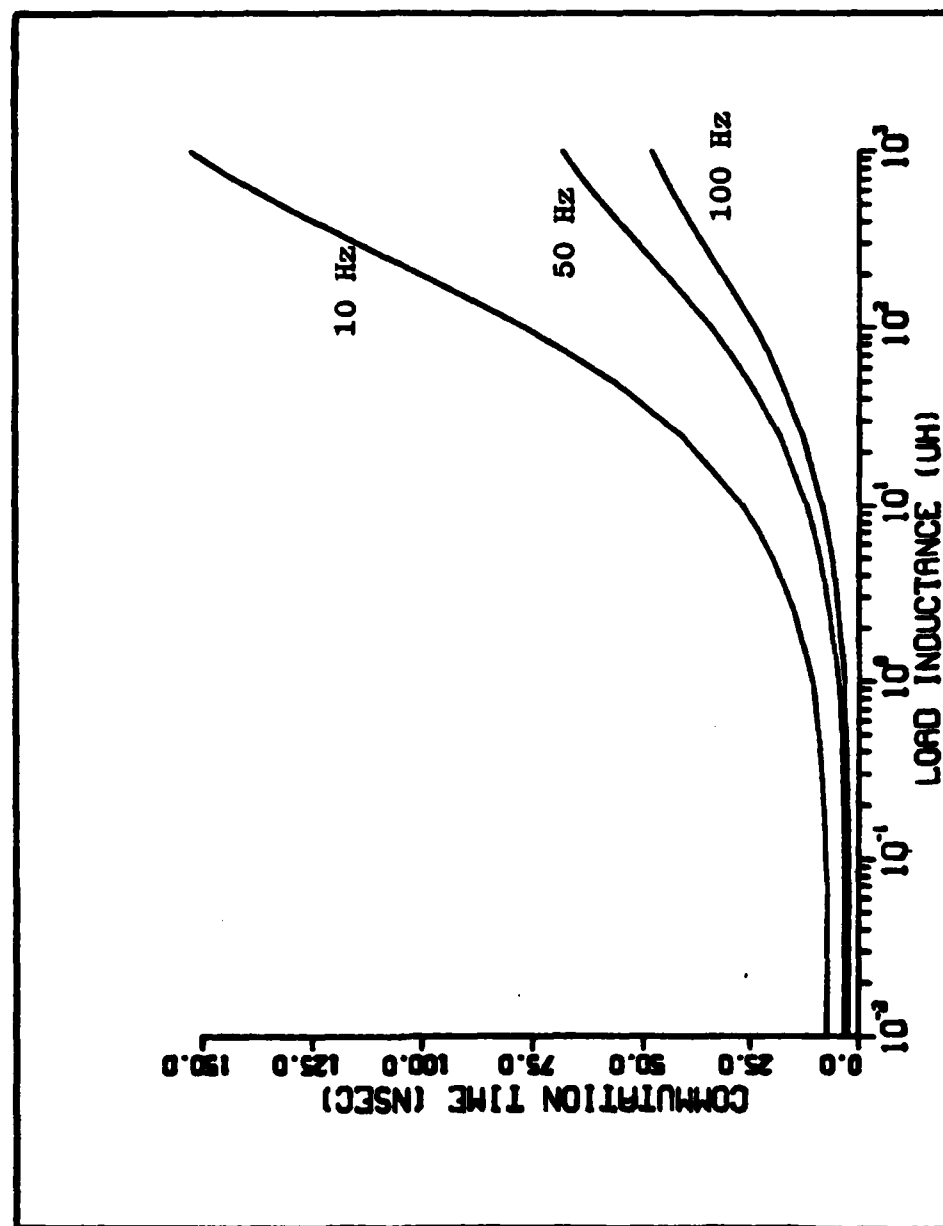


Figure 15. Commutation Time vs. Load Inductance as a Function of Switching Frequency

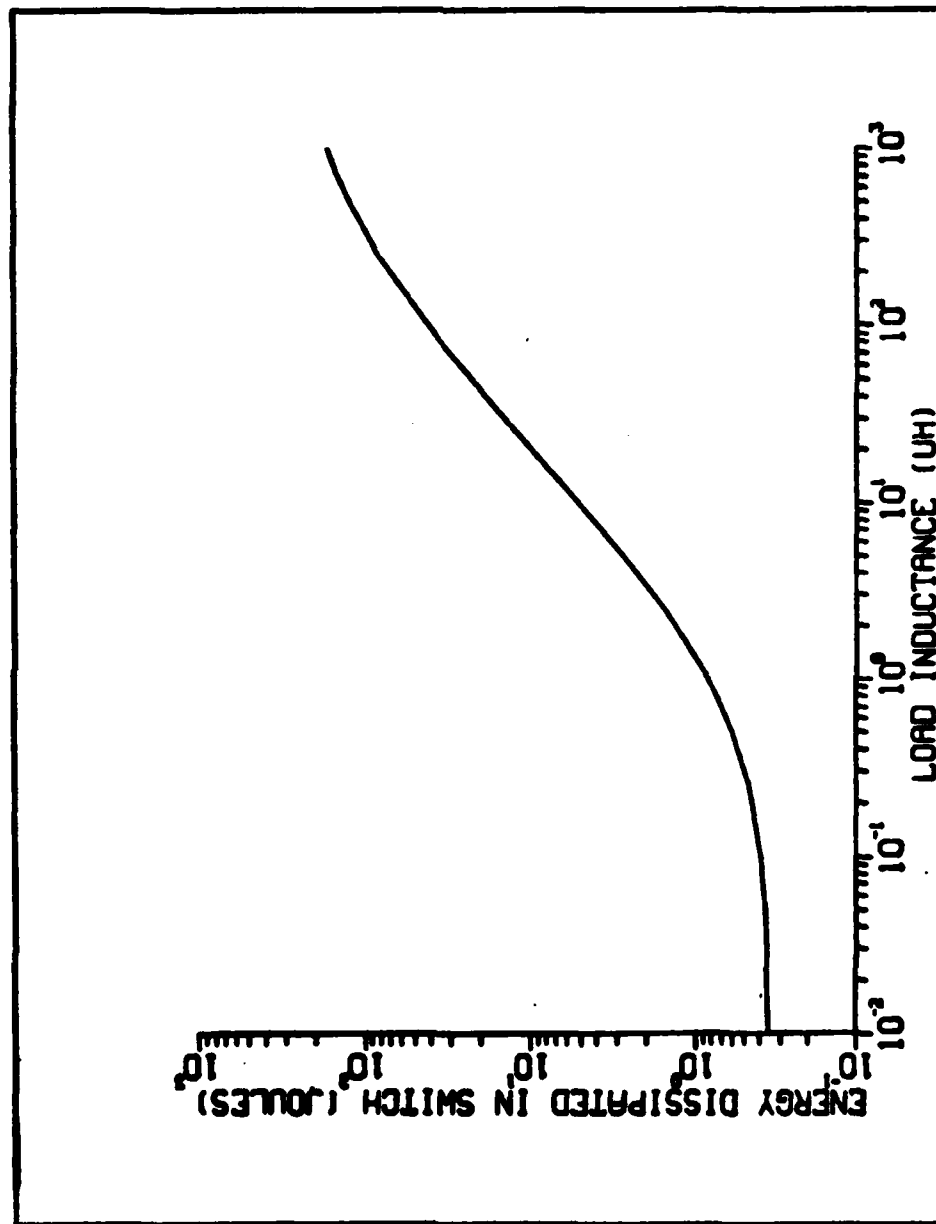


Figure 16. Energy Dissipated in the Switch vs. Load Inductance for an Initial Current of 1 kA

V. Results

Introduction

Almost 100 switch tests were run using the new rotor and brush designs. This chapter summarizes the results of those tests. After comparing the switching capabilities of the original and new rotors, the commutating characteristics of each of the new brush designs is discussed.

Results

Rotor Comparisons. The original rotor had a copper-epoxy interface at the edge of the insulating slot. Figure 17 shows the load current and load voltage pulses resulting from a typical switching event using the original rotor and six standard brushes. The figure depicts one pulse out of seven which occurred during a particular run. The power supply was set at 2 kA and the switching frequency was 8 Hz. The average load current and load voltage for the test were 1.98 kA and 16.5 V, respectively. The average pulse length was 12.1 mS, resulting in a .9 duty cycle (ratio of coil charge time to total cycle time). The

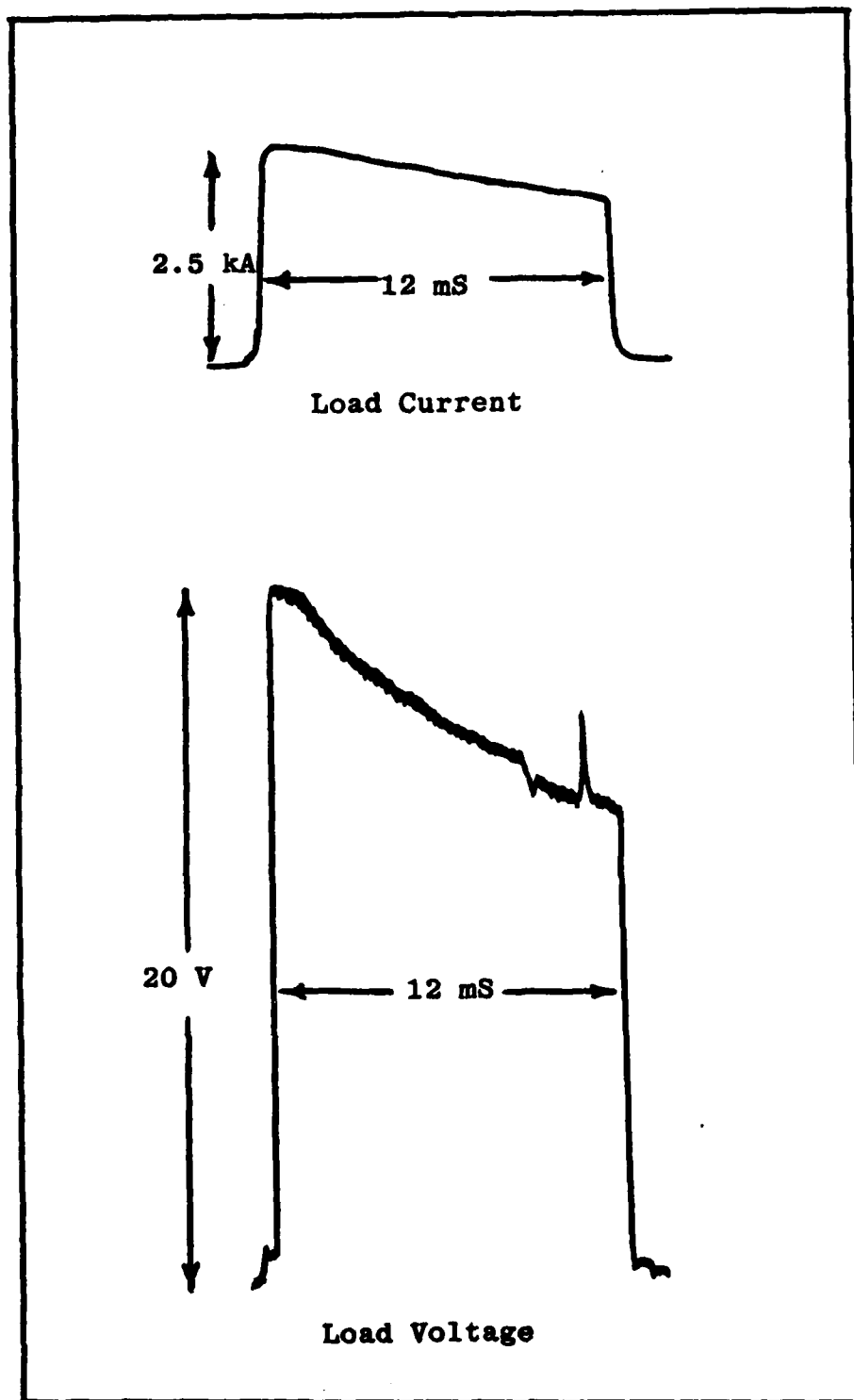


Figure 17. Typical Load Current and Voltage Pulses Resulting from the Original Rotor

average energy delivered to the load was .43 kJ per pulse and a total of 3 kJ was delivered to the load during the seven pulses.

The load current and load voltage pulses shown in Figure 17 were recorded at 160 in/sec, the fastest visicorder chart speed. Therefore, further expansion of the pulses to obtain more detail about the rising and trailing edges of the pulses was not possible. The small step at the bottom of the leading edge of both pulses is probably due to arcing during the commutating phase. The slope on the top portion of the current pulse and the irregularities on the top portion of the voltage pulse were introduced by the ripple and variations associated with the power supply.

It should be kept in mind that Figure 17 (and other figures of pulses in this thesis) was traced by hand from the Honeywell Visicorder oscillographs and all of the original detail could not be exactly reproduced since several small excursions on the oscillograph could occur within the width of a line in the figure. However, the figure does illustrate a very close representation of the original pulse

Figure 18 shows a typical load current and load voltage pulse resulting from the new rotor with tungsten inserts placed at the copper-epoxy interface. For this switching event (run number 12, Table II), the power supply was set at

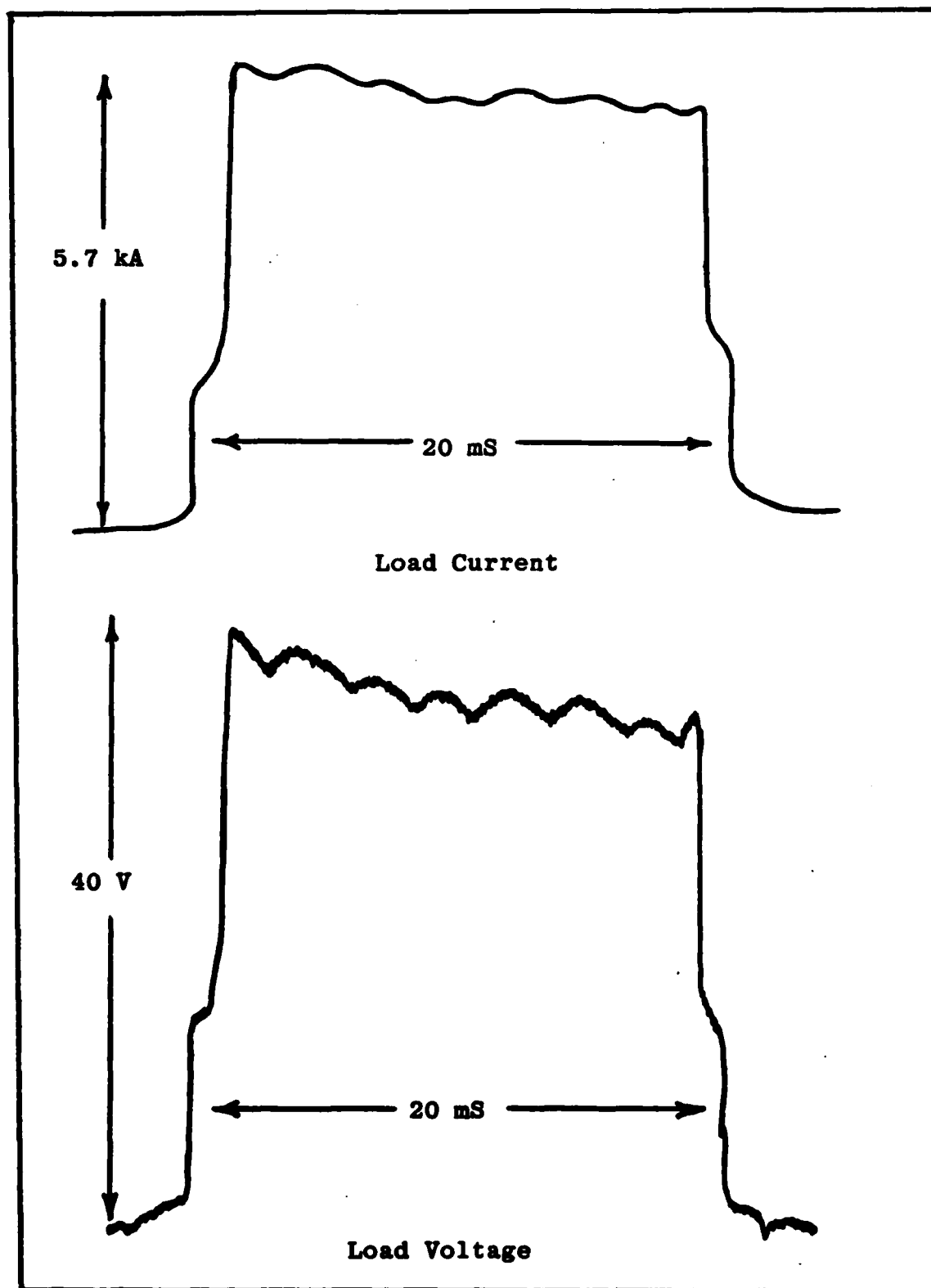


Figure 18. Typical Load Current and Voltage Pulses Resulting from the New Rotor

6 kA and the switching frequency was 4.68 Hz. The average load current was 5.51 kA and the average load voltage was 36.4 V. The average pulse width was 21.6 mS resulting in a .9 duty cycle. The average pulse energy was 4.33 kJ, while a total of five pulses delivered 21.66 kJ to the load during the test run.

The initial step in the rising edge of the pulses is probably due to the brushes sliding from the copper section onto the tungsten inserts. The large second step is probably due to the brushes sliding onto the tungsten inserts and the epoxy insulating slot. The initial slope of the final jump probably results from the stretching of the arc while the steepest slope represents a complete commutation of current into the load. The trailing edge of the pulse is very similar to the rising edge of the pulse since the switching process is merely reversed. The only difference is that the arc is not present.

Comparing Figure 18 with Figure 17, it can be seen that setting the power supply on a higher current setting (6 kA versus 2 kA) significantly reduces the ripple in the current and voltage waveforms.

Table II shows the results of the first 33 test runs using standard brushes on the new rotor. The table consists of switching data tabularized according to the run number. Six brushes were used during each of the runs and a total of

Table II-A

New Rotor Switching Data Using Standard Brushes

Run Number	Set Current (kA)	Average Switch Current (kA)	Average Current per Brush (kA)	Average Load Current (kA)	Average Switch Voltage (V)	Average Load Voltage (V)
1	2.0	1.85	.62	1.82	.56	15.3
2	2.0	2.2	.73	2.2	.56	16.3
3	2.0	1.94	.65	1.86	.56	15.5
4	2.0	1.67	.56	1.67	.56	14.7
5	2.0	1.41	.47	1.44	.48	14.4
6	4.0	2.13	.71	2.05	.56	8.8
7	4.0	4.22	1.41	4.03	.48	14.6
8	4.0	4.1	1.37	3.91	.72	13.6
9	2.0	1.44	.48	1.18	.72	11.2
10	2.0	1.67	.56	1.71	.64	15.6
11	2.0	1.94	.65	2.05	.96	17.6
12	6.0	5.66	1.89	5.51	2.72	36.4
13	6.0	6.19	2.06	5.85	2.68	39.6
14	6.0	6.15	2.05	5.93	2.84	41.6
15	6.0	6.16	2.05	5.55	2.76	38.2
16	6.0	6.16	2.05	5.59	2.8	38.2
17	6.0	6.1	2.03	5.78	3.4	40.6
18	6.0	6.19	2.06	5.78	3.2	40.4
19	6.0	6.19	2.06	5.78	3.96	42.
20	6.0	5.93	1.98	5.74	3.76	41.6
21	.3	.65	.22	.38	.4	3.4
22	.5	.59	.2	.49	.64	4.8
23	.5	.61	.2	.49	--	6.0
24	1.0	1.18	.39	1.35	--	13.2
25	2.0	2.05	.68	1.82	--	16.4
26	3.0	3.0	1.	2.85	--	24.
27	4.0	4.6	1.53	4.65	--	36.8
28	5.0	6.08	2.03	5.5	--	42.
29	5.0	6.46	2.15	6.16	--	46.
30	5.0	6.42	2.14	6.04	--	46.
31	6.0	6.66	2.22	6.19	--	48.
32	6.0	6.57	2.19	6.28	--	53.
33	6.0	6.43	2.14	5.7	--	45.

Table II-B

New Rotor Switching Data Using Standard Brushes

Run Number	Frequency (Hz)	Pulse Width (mS)	Duty Cycle	Average Pulse Energy (kJ)	Number of Pulses	Total Energy (kJ)
1	19.42	5.	.9	.139	30	4.18
2	19.7	5.1	.9	.183	13	2.38
3	4.85	21.	.9	.605	3	1.82
4	4.68	19.8	.9	.487	4	1.95
5	59.2	1.7	.9	.035	56	1.97
6	58.8	1.6	.9	.029	22	.64
7	20.	5.	.9	.294	17	5.
8	5.34	19.4	.9	1.03	4	4.13
9	4.51	21.	.9	.278	5	1.39
10	4.5	21.	.9	.56	7	3.92
11	4.65	22.	.9	.794	8	6.35
12	4.68	21.6	.9	4.33	5	21.66
13	20.3	5.6	.89	1.3	37	48.
14	60.1	1.4	.92	.345	62	21.4
15	5.9	16.	.9	3.39	7	23.75
16	5.93	16.	.9	3.42	3	10.25
17	61.2	1.5	.9	.352	74	26.05
18	23.3	4.5	.9	1.05	22	23.12
19	58.8	2.0	.88	.491	64	31.45
20	60.6	1.5	.91	.358	26	9.31
21	5.26	18.	.91	.023	4	.093
22	20.	4.5	.91	.011	18	.191
23	18.5	5.	.91	.015	8	.118
24	18.2	4.9	.91	.087	19	1.66
25	18.2	4.5	.92	.134	16	2.15
26	18.2	4.5	.92	.308	14	4.31
27	18.2	4.5	.92	.768	19	14.6
28	20.4	4.2	.91	.97	12	11.64
29	20.4	4.	.91	1.13	11	12.47
30	59.9	1.2	.93	.333	66	22.
31	22.8	4.	.91	1.19	21	24.96
32	59.9	1.2	.93	.399	48	19.17
33	5.59	15.7	.91	4.03	6	24.16

731 commutations occurred without a single failure.

During runs 15 through 20, the stainless steel plate load configuration was shifted further out on the buss bars to increase the load inductance and obtain a higher load voltage. A three-turn loop was connected to the load to further increase the load inductance for runs 21 through 33. The resulting spike on the leading edge of the load voltage pulse ranged from about 1 V up to a maximum value of 88 V. The new rotor handled the increased voltage without any problem. A slight decrease in the load current pulse width was noticed due to the increased inductance.

In general, the new rotor was successful. As seen in Figure 18, the higher resistivity of the inserts did reduce the current available for arcing during the commutating phase since it had already been switched into the load. Although this does not prevent arcing, it does reduce the severity of the arc-related damage and increase the lifetime of the rotor.

Although the tungsten-epoxy boundary did show some signs of damage from the commutation process, it was much less than the damage on the original rotor without the inserts. The main problem appeared to be a narrow gap which formed at the tungsten-epoxy interfaces. This gap resulted in minor brush bounce as the brushes crossed the surface discontinuity.

Fringe Fiber Brush Design. The results of twenty test runs using fringe fiber brushes on the new rotor are shown in Table III. Only two brushes were used during the initial ten runs while the remaining runs had a full complement of ten brushes. The loop previously mentioned for increasing the load inductance was connected during runs 1 through 16 and disconnected for the remaining four runs.

It is interesting to note that increasing the number of brushes from two in run number 10 to ten in run number 11 decreased the brush contact voltage by almost 40%. This verifies that a larger number of contact points decreases the brush contact resistance, resulting in a smaller brush contact voltage drop.

A typical load current and load voltage pulse from run number 3 is shown in Figure 19. The initial step in the current pulse is due to the higher resistance of the tungsten inserts while the sloped pulse top is due to the power supply ripple. The exponential decay of the trailing edge of the pulse is a result of the time constant associated with the load inductance and resistance. The average current during the pulse was .466 kA and the switching frequency was 5.4 Hz.

The shape of the voltage pulse in Figure 19 was as anticipated. The spike of 16.6 V is a result of the increased load inductance while the average value was 5.2 V.

Table III-A

New Rotor Switching Data Using Fringe Fiber Brushes

Run Number	Set Current (kA)	Average Switch Current (kA)	Average Current per Brush (kA)	Average Load Current (kA)	Average Switch Voltage (V)	Average Load Voltage (V)
1	.5	.38	.38	.35	.24	3.4
2	.5	.67	.67	.5	.4	5.2
3	.5	.59	.58	.47	.36	5.2
4	.5	.6	.6	.66	.36	7.0
5	1.0	--	--	1.14	.56	10.4
6	1.0	--	--	1.38	--	14.4
7	1.0	--	--	1.12	--	16.
8	1.5	1.88	1.88	1.79	.56	16.
9	1.5	1.81	1.81	1.15	.6	11.
10	2.0	1.63	1.63	1.9	.72	16.
11	2.0	1.6	.32	1.48	.44	13.8
12	2.0	1.62	.32	1.59	.4	16.
13	2.0	1.75	.35	1.6	.44	15.
14	4.0	4.28	.86	4.57	.9	32.
15	6.0	6.28	1.26	6.1	--	47.5
16	8.0	7.52	1.50	7.43	--	55.
17	2.0	1.74	.35	1.81	.48	15.
18	2.0	1.84	.37	1.81	.56	16.4
19	4.0	4.57	.91	4.43	.83	33.
20	6.0	6.62	1.32	6.4	--	46.

Table III-B

New Rotor Switching Data Using Fringe Fiber Brushes

Run Number	Frequency (Hz)	Pulse Width (mS)	Duty Cycle	Average Pulse Energy (kJ)	Number of Pulses	Total Energy (kJ)
1	20.4	5.	.9	.006	15	.09
2	20.5	4.8	.9	.012	1	.012
3	5.4	18.4	.9	.044	2	.089
4	60.2	2.	.88	.063	11	.695
5	5.44	17.7	.9	.209	4	.839
6	17.9	4.8	.91	.095	16	1.53
7	--	1.8	--	.032	24	.774
8	6.1	16.5	.9	.473	10	4.73
9	6.1	15.8	.9	.2	12	2.4
10	6.12	16.0	.9	.486	15	7.3
11	5.	20.	.9	.408	7	2.86
12	5.05	18.6	.91	.473	10	4.73
13	20.4	4.6	.91	.11	31	3.42
14	20.4	4.5	.91	.658	37	24.35
15	21.5	3.8	.92	1.1	36	39.64
16	20.6	3.7	.92	1.5	35	52.92
17	21.3	5.0	.89	.136	15	2.04
18	20.6	4.6	.91	.137	45	6.14
19	20.7	4.35	.91	.636	34	21.62
20	20.7	4.3	.91	1.27	35	44.31

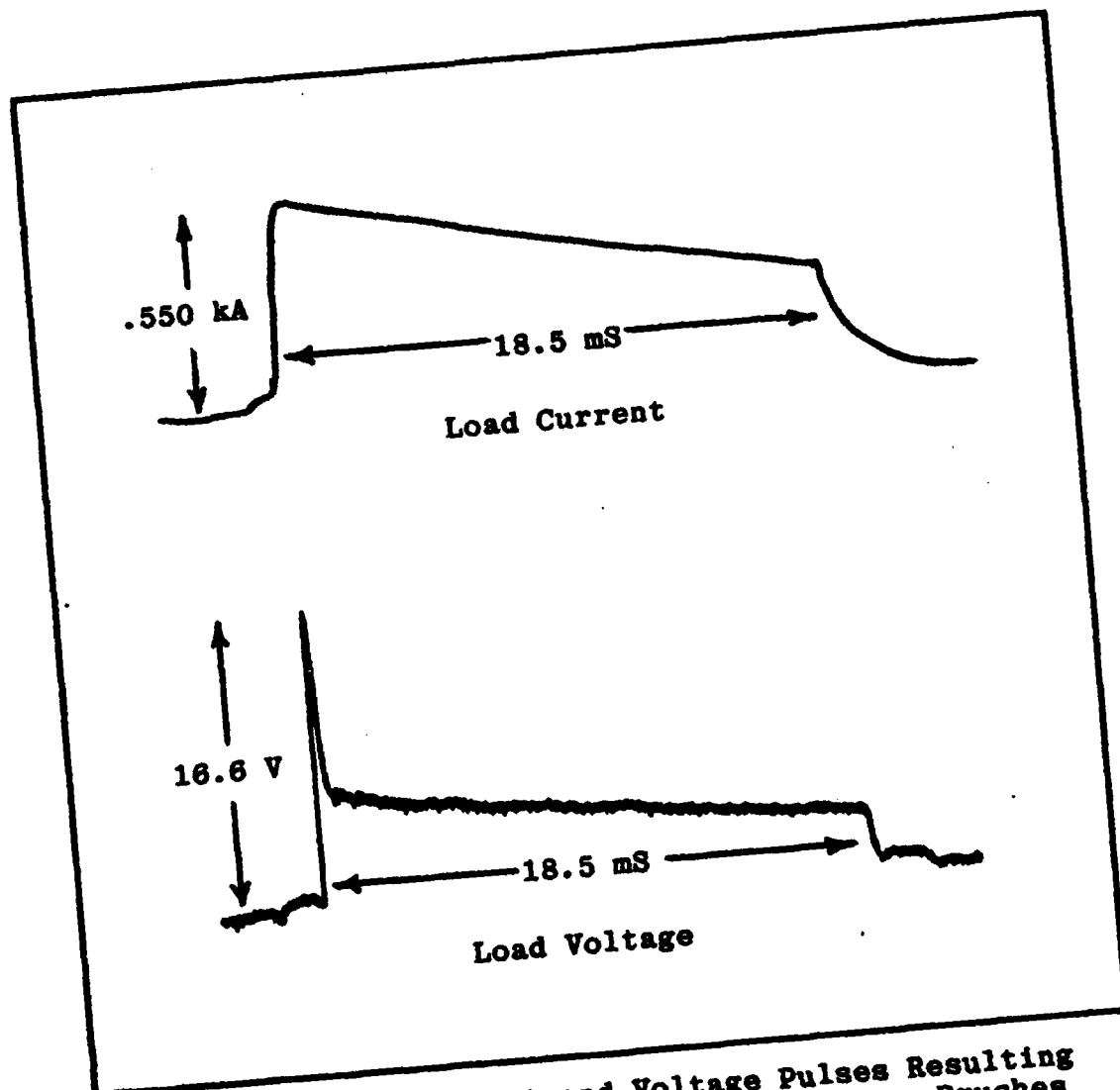


Figure 19. Load Current and Voltage Pulses Resulting from the New Rotor, Fringe Fiber Brushes and a High Inductive Load

The fringe fiber brush design did not provide the resistive commutation which was expected. It is believed that the following commutation process occurred. As the current in the brush (up to 1.88 kA) flowed into the carbon fibers, the conductive cement which connected the fibers to the brush began to carbonize and the fibers began to unfasten themselves from the brush. Once the arc was established between the fibers and the rotor surface, the stretching of the arc tugged on the woven fibers pulling them apart and even separating them from the brush at times. The fibers on the leading edge of the brush remained intact since they were not subjected to any arcing. Figure 7 shows six fringe fiber brushes. The three brushes which are not connected to brush straps (center of photo) have not been tested. The three brushes connected to the straps were used to obtain the data in Table III. Note how the fibers on the trailing edge of the brushes have been pulled away from the brush.

Finger Brush Design. The switching data resulting from twenty-six test runs using the finger brushes on the new rotor is shown in Table IV. Six brushes were used during runs 1 through 19 and ten brushes were used during runs 20 through 26.

The highest average current which the switch could conduct without failure was 6.28 kA (run number 9). This

Table IV-A

New Rotor Switching Data Using Finger Brushes

Run Number	Set Current (kA)	Average Switch Current (kA)	Average Current per Brush (kA)	Average Load Current (kA)	Average Switch Voltage (V)	Average Load Voltage (V)
1	2.0	1.63	.543	1.5	.56	16.
2	2.0	1.56	.52	1.59	.48	15.
3	2.0	1.57	.523	1.49	.44	13.5
4	2.0	1.6	.533	1.59	.44	15.8
5	2.0	1.66	.553	1.71	.56	16.
6	2.0	1.7	.567	1.63	.48	16.
7	4.0	4.08	1.36	4.48	.63	34.2
8	6.0	5.71	1.903	5.76	1.0	54.
9	6.0	6.28	2.093	6.12	1.9	44.5
10	2.0	1.4	.467	1.75	.48	14.6
11	2.0	1.56	.52	.665	.65	6.4
12	4.0	2.51	.837	2.24	.96	17.6
13	2.0	--	--	--	--	--
14	2.0	1.9	.633	1.52	.48	14.4
15	4.0	3.71	1.237	3.71	1.1	30.
16	2.0	--	--	--	--	--
17	2.0	1.67	.557	1.63	1.12	16.5
18	4.0	3.81	1.27	3.5	1.92	39.
19	5.0	5.79	1.93	5.71	--	41.
20	2.0	1.92	.384	2.03	.3	15.6
21	2.0	2.09	.418	2.41	--	18.6
22	2.0	2.28	.456	2.36	.72	19.
23	4.0	4.18	.836	4.71	1.1	29.2
24	4.0	4.28	.856	4.57	1.4	33.
25	4.0	--	--	5.4	1.8	44.
26	4.0	3.71	.742	4.21	1.4	31.

Table IV-B

New Rotor Switching Data Using Finger Brushes

Run Number	Frequency (Hz)	Pulse Width (mS)	Duty Cycle	Average Pulse Energy (kJ)	Number of Pulses	Total Energy (kJ)
1	20.	5.	.9	.12	30	3.6
2	20.6	5.	.9	.119	35	4.17
3	20.2	5.	.9	.1	24	2.41
4	20.4	5.	.9	.126	29	3.64
5	20.4	5.	.9	.137	27	3.69
6	20.8	5.	.9	.13	26	3.39
7	20.5	4.8	.9	.74	25	18.39
8	20.9	4.5	.91	1.4	14	19.6
9	20.4	4.6	.91	1.25	28	35.08
10	5.6	17.	.9	.434	4	1.74
11	5.45	17.8	.9	.076	14	1.06
12	5.62	17.7	.9	.698	11	7.68
13	5.9	--	--	--	3	--
14	5.8	16.2	.91	.355	12	4.26
15	5.95	16.4	.9	1.83	15	27.38
16	--	--	--	--	208	--
17	62.5	2.	.88	.054	60	3.23
18	61.3	1.6	.9	.218	85	18.56
19	60.8	1.5	.91	.351	40	14.05
20	5.62	17.5	.9	.827	8	6.62
21	20.	4.5	.91	.202	40	8.07
22	35.3	2.8	.9	.126	45	5.65
23	5.52	16.5	.91	2.27	9	20.42
24	19.6	5.	.9	.754	28	21.1
25	60.2	1.3	.92	.309	55	16.99
26	20.	5.	.9	.652	15	9.79

was the equivalent of 2.093 kA per brush. During this run, the "fingers" melted and the solder which connected the brushes to the brush straps softened. This resulted in the top three brushes separating from the brush straps. The pressure from the actuator pistons forced the brush straps against the rotor surface resulting in a partial melting of the strap ends. The top surface of the rotor was covered with burn marks from arcing. Some pitting and solder blotches could also be found around the rotor surface. The bottom set of brushes remained attached to the straps and the fingers had not melted. The bottom side of the rotor had several burn marks from arcing but it was not as severe as the top side.

Once a new set of six finger brushes was made, testing resumed with run number 10. During run number 19, the brushes once again failed. This time the average current through the switch was 5.79 kA or 1.93 kA per brush. The results were basically the same as run number 9 with the exception that two of the bottom three brushes also separated from the brush straps.

A set of ten finger brushes was then constructed. In addition to soldering the brushes to the straps, small set screws (like those shown in Figure 7) were screwed into the brush straps to anchor the finger brushes onto the straps. It was hoped that this would prevent the brushes from

separating from the straps. These brushes were tested from run number 20 to run number 26.

During run number 26, the "fingers" on the top brushes melted while conducting an average current of only 3.71 kA or .742 kA per brush. However, none of the brushes separated from the brush straps. After the brush straps were removed from the mounts it was discovered that two of the top brushes were fused together from the melted copper and solder.

During this run, an interesting phenomenon occurred. Although all five of the top brushes were partially melted and the top rotor surface was covered with burn marks, the bottom five brushes remained completely intact, showing no signs of melting and the bottom rotor surface had only one minor burn mark! The most probable reason for the vast difference between the performance of the top and bottom brushes is related to the solder connection between the brushes and the brush straps. As solder melted on the top brushes it flowed down the "fingers" and onto the rotor surface, resulting in catastrophic effects. On the other hand, as solder melted on the bottom set of brushes, it could not flow up onto the rotor surface. Instead, it remained in the area of the original solder joint and did not hinder the performance of the bottom brushes.

The purpose of the brush "fingers" was to increase the number of contact points at the brush-rotor surface interface, effectively decreasing the brush contact resistance and voltage drop. However, this was not the case. Comparing the switch voltage drop of the finger brushes with the switch voltage drop of the standard and fringe fiber brushes at equal current levels, no improvement was found.

One possible explanation is that all of the "fingers" were not touching the rotor surface. For example, the "fingers" left track marks on the rotor surface where contact was being made. Despite initially wearing in the brush "fingers" evenly by placing a fine sandpaper on the rotor surface, the number of "finger" tracks on the rotor surface was typically less than the number of "fingers" across the brush. This indicated that all of the "fingers" were not necessarily making contact.

Since the "fingers" tended to dig into the rotor surface, the rotor experienced more surface wear from these brushes than from the standard and fringe fiber brushes. The epoxy insulating slot had deeper track marks than the copper section since it was not as hard as the copper section. This presented some problems at the second tungsten-epoxy interface.

A small step had to be surmounted by the brushes as they transitioned from the epoxy section onto the tungsten inserts. As a result, the brushes bounced, continuing to commutate current into the load and a distinct trailing edge on the load current pulse was no longer possible. Figure 20 shows several examples of load current pulses resulting from the brush bounce. Figure 20-(a) was obtained from run number 17 where the switching frequency was 62.5 Hz and the average load current was 1.63 kA.

Figure 20-(b) occurred during run number 18 where the switching frequency was 61.3 Hz and the average load current was 3.5 kA. The average rotor surface speed for Figure 20 was approximately 60 m/sec.

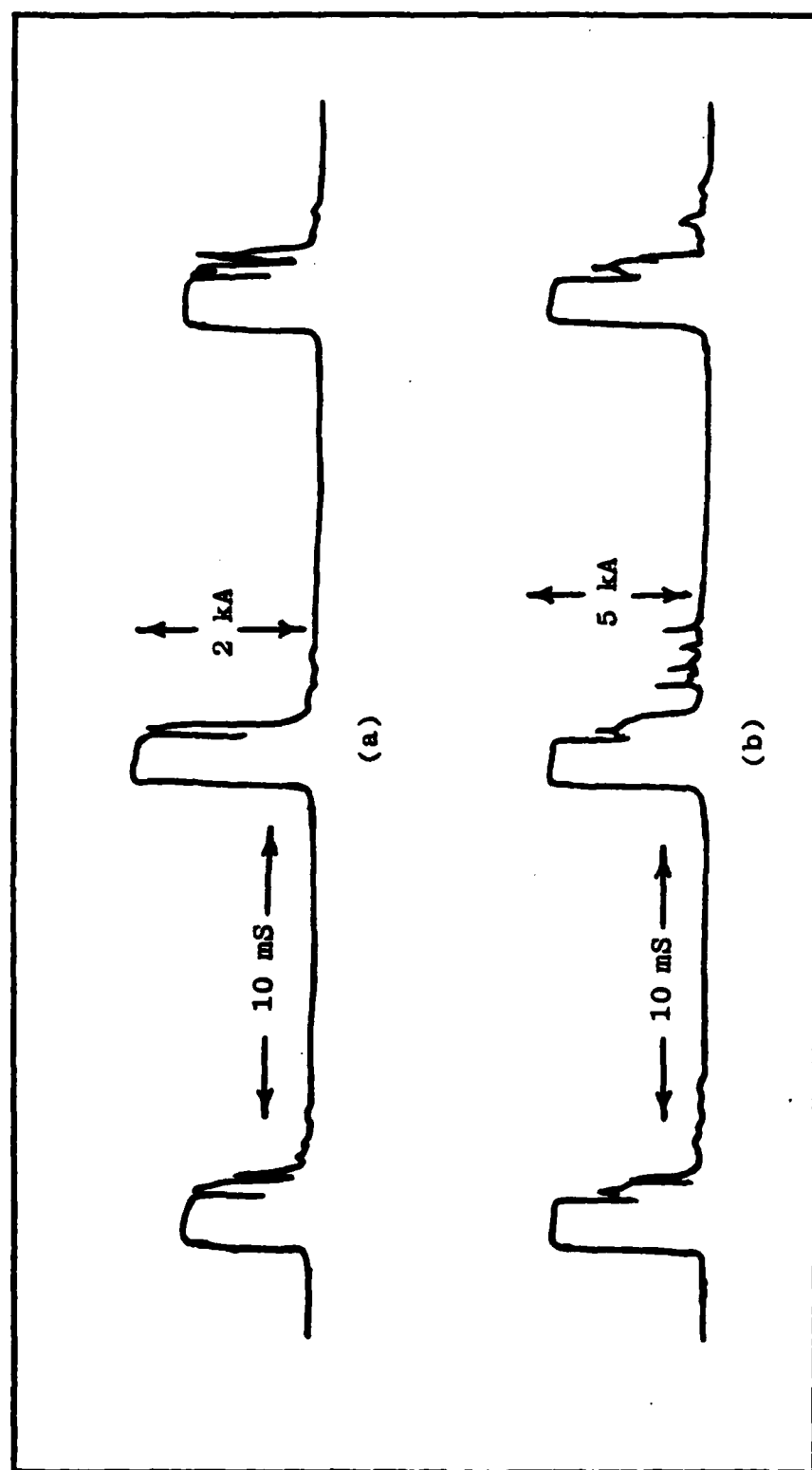


Figure 20. Load Current Waveforms Showing the Effects of Brush Bounce

VI. Conclusions and Recommendations

The new rotor was very successful. It commutated current more than 2,400 times without a single rotor-related failure. It achieved a maximum switching rate of 62.5 Hz and conducted a maximum average current of 7.52 kA. Higher current levels were limited by the power supply output. The new rotor also handled load voltages up to 136 V without any problem. Resistive commutating action due to the presence of the tungsten inserts was observed and the arc-related damage was reduced when compared with the original rotor.

The fringe fiber and finger brush designs were not successful at current levels above 4 kA. The major problem was with the solder which held the brushes to the brush straps and the conductive cement which connected the carbon fibers to the brushes. As the solder melted and flowed into the "fingers" of the finger brushes, the "fingers" melted and, in some cases, the brushes separated from the straps. As the conductive cement carbonized on the fringe fiber brushes, the carbon fibers were tugged away from the brush and completely separated in some instances.

Since the brushes appear to be the major drawback for switching high currents, it is recommended that research in

this area continue. Figure 21 shows a new brush design which may improve the commutating process. Figure 21-(a) shows the expected current flow lines as current flows through a standard brush and the rotor. For simplicity, it is assumed that the brush contact resistance is uniform across the brush-rotor interface. As the brush slides onto the insulator section [Figure 21-(b)], the current density increases toward the trailing edge of the brush. As a result, the current continues to flow through the rotor instead of starting its commutation process into the load. Figure 21-(c) shows a new brush design where current is "channeled" through the brush. The "channeling" effect is accomplished by placing insulating spacers between the conducting sections of the brush. As this brush passes over the insulator section [Figure 21-(d)], the current can not easily diffuse toward the trailing edge of the brush due to the presence of the insulating spacers. Thus current commutation starts earlier, enhancing the commutation process and reducing the amount of current available for arcing.

Figures 21-(c) and (d) show a possible brush strap configuration for mounting the new brush design. This technique uses a small bolt to fasten the brush to the brush strap instead of solder, reducing the likelihood of solder-related brush failure.

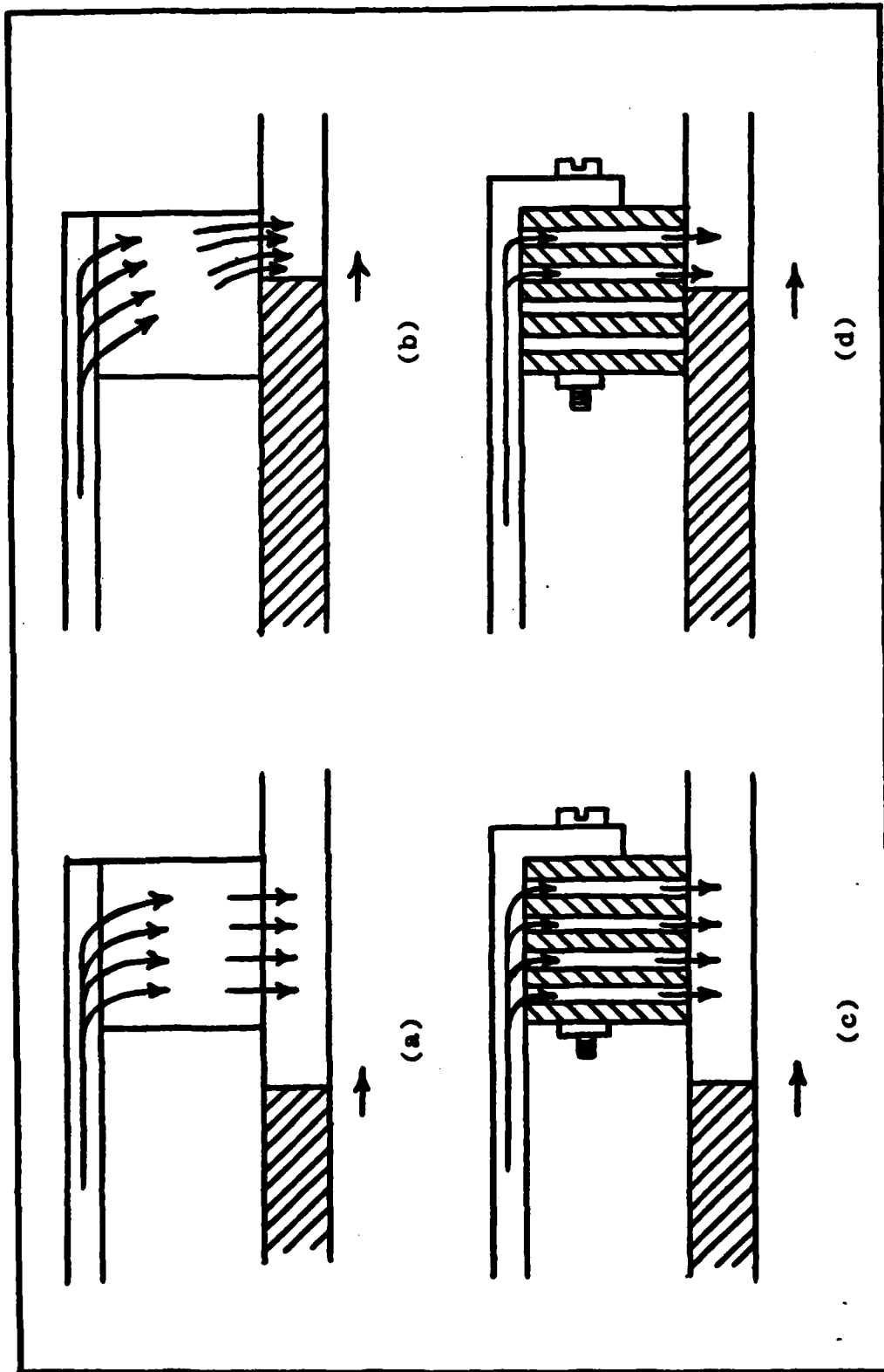


Figure 21. Current Flow Through a Standard Brush and Through a New Brush Design During Commutation

Other recommended areas of rotary switch research include cooling the brushes with liquid nitrogen or hydrogen, running the switch in different environments such as sulfur hexafluoride (SF_6) and finding a new way to mount the brushes which eliminates the use of solder. Finally, it is recommended that a material harder than epoxy resin be used for the insulator slot. A harder material would reduce the surface wear associated with brush designs similar to the finger brushes and tremendously reduce the brush bounce at the trailing edge of the pulse.

Bibliography

1. Kristianson, M. "Fundamentals of Inductive Energy Storage." Workshop on Repetitive Opening Switches, January 28-30, 1981. AD-A110770.
2. Barber, John P., et al. "Electromagnetic Gun Study." AFATL-TR-81-82. Eglin AFB, FL, 1981.
3. Barber, John P. and Bauer, David P. "Repetitive Switching for Electric Rail Guns." IAP-TR-82-8. Dayton OH, December, 1982.
4. Clark, Capt Gerald P. Project Engineer, Aero Propulsion Laboratory (personal communication). Wright-Patterson AFB, OH, July, 1983.
5. Barber, John P. and Trzaska. "Repetitive Switching for Inductive Energy Storage." AFWAL-TR-82-2088. Wright-Patterson AFB, August, 1982.
6. Windred, George. Electrical Contacts, MacMillan and Co. Limited, St. Martin's Street, London, 1940.
7. Swinnerton, B. R. G. "Carbon Fibre Fringe Brush." Advances in Electrical Current Collection, 1982.
8. Baurer, David P., et al. "Electric Rail Gun Propulsion Study (Advanced Electric Propulsion Technology - High Thrust)." AFRPL-TR-81-02. Edwards AFB, CA, 1981.

Appendix A
Computer Program

Program Switch

This program will compute the time required to commutate current using an opening switch with characteristics of the rotary switch previously mentioned in the thesis. The current level, switching frequency, load inductance and output interval are input values which are entered from the terminal. Once the program has been executed, the output consists of a tabulation of the switch resistance, switch current, load current, switch voltage and energy dissipated in the switch, all as a function of time. Plots of switch current versus time and switch voltage versus time as a function of three switching frequencies can be obtained using the DISSPLA plotting routine provided that the same current level is entered for each plot, the switching frequency increases with each consecutive plot, and a Tektronics terminal is used.

The program variables are as follows:

RC	- coil resistance
RS	- switch resistance
RL	- load resistance
LC	- coil inductance
LS	- switch inductance
LL	- load inductance

IO	- initial current level
I1	- current flowing in the coil-switch loop
I2	- current flowing in the load-switch loop
IS	- total current flowing through the switch (I1 - I2)
ISF	- final value of switch current (when this value is reached, the program stops)
SWFREQ	- rotor switching frequency
T	- time
WS	- energy dissipated in the switch
LV	- load voltage (equal to the switch voltage)
DI1	- incremental value of I1
DI2	- incremental value of I2
DT	- incremental value of time
DRS	- incremental value of switch resistance
DWS	- incremental value of energy dissipated in the switch
COUNT	- a counter which increments up to the output interval value and then resets to 0
OUTINT	- the number of iterations which occur before the tabular output is printed (output interval)
NOPLT	- number of plots (must equal 3.0)
LVPINC	- load voltage plotting increment (tic mark on graph)
TPINC	- time plotting increment
ISPINC	- switch current plotting increment

LVPMAX	- maximum load voltage plotted
TPMAX	- maximum time plotted
ISPMAX	- maximum switch current plotted
IND	- index for the array location
TP1, TP2, TP3	- arrays storing the time values to be plotted on each of the three graphs
ISP1, ISP2, ISP3	- arrays storing the switch current values to be plotted on each of the three graphs
LVP1, LVP2, LVP3	- arrays storing the load voltage (equal to the switch voltage) values to be plotted on each of the three graphs

The remainder of Appendix A contains the computer program listing followed by a sample tabular output. The corresponding plots of switch current and voltage versus time are shown in Figures 12 and 13 of the text.

PROGRAM SWITCH

* THIS PROGRAM WILL COMPUTE THE TIME REQUIRED TO
* COMMUTATE CURRENT USING AN OPENING SWITCH IN AN
* INDUCTIVE ENERGY STORAGE CIRCUIT. THE OUTPUT
* CONSISTS OF A TABULATION OF SWITCH RESISTANCE,
* SWITCH CURRENT, LOAD CURRENT, SWITCH VOLTAGE,
* AND ENERGY DISSIPATED IN THE SWITCH, ALL AS A
* FUNCTION OF TIME. IF THE PROGRAM IS EXECUTED
* ON A TEKTRONICS TERMINAL, PLOTS OF SWITCH CUR-
* RENT AND VOLTAGE VS TIME CAN BE OBTAINED USING
* THE DISSPLA PLOTTING ROUTINE.

```
REAL RC,RS,RL,LC,LS,LL
REAL IO,I1,I2,IS,ISF,SWFREQ,T,WS,LV
REAL DI1,DI2,DT,DRS,DWS
REAL COUNT,OUTINT,NOPLT
REAL LVPINC,TPINC,LVPMAX
REAL ISPINC,ISPMAX,TPMAX
REAL TP1(60),ISP1(60),LVP1(60)
REAL TP2(60),ISP2(60),LVP2(60)
REAL TP3(60),ISP3(60),LVP3(60)
```

* ESTABLISH THE CIRCUIT COMPONENT VALUES AND THE
* NUMBER OF PLOTS (NOPLT MUST EQUAL 3.0).

```
RC=7.85E-3
RL=27.0E-3
LC=5.0E-4
LS=0.7E-6
NOPLT=3.0
```

* ENTER FROM THE TERMINAL THE INITIAL CURRENT
* LEVEL, SWITCHING FREQUENCY, LOAD INDUCTANCE,
* AND THE OUTPUT INTERVAL FOR THE TABULATED DATA.

```
10 PRINT*,'ENTER THE CURRENT LEVEL IN AMPS: '
   READ*,IO
   ISF=10*0.001

   PRINT*,'ENTER THE SWITCHING FREQUENCY IN HERTZ: '
   READ*,SWFREQ

   PRINT*,'ENTER THE LOAD INDUCTANCE IN HENRIES: '
   READ*,LL

   PRINT*,'ENTER THE OUTPUT INTERVAL: '
```

READ*,OUTINT

* ESTABLISH THE TIME STEP AND INITIAL CONDITIONS.

DT=1.0E-12
IND=1
I1=I0
ISPMAX=I0/1000.
I2=0.0
DI1=0.0
DI2=0.0
RS=0.0
DRS=0.0
WS=0.0
T=0.0
COUNT=0.0
IS=I1-I2
LV=0.0

* PLACE THE INITIAL CONDITIONS INTO THE ARRAYS
* WHICH WILL BE USED LATER FOR PLOTTING.

IF(NOPLT.EQ.3.0) THEN
TP1(IND)=0.0
ISP1(IND)=ISPMAX
LVP1(IND)=0.0
END IF

IF(NOPLT.EQ.2.0) THEN
TP2(IND)=0.0
ISP2(IND)=ISPMAX
LVP2(IND)=0.0
END IF

IF(NOPLT.EQ.1.0) THEN
TP3(IND)=0.0
ISP3(IND)=ISPMAX
LVP3(IND)=0.0
END IF

PRINT 2000
2000 FORMAT(/,6X,'T',9X,'RS',9X,'IS',9X,'I2',9X,
>'LV',9X,'WS',/)
PRINT 3000,T,RS,IS,I2,LV,WS
3000 FORMAT(1X,E9.4E1,5(2X,E9.4E1))

* BEGIN THE FINITE DIFFERENCE METHOD, PLACING
* OUTPUT DATA INTO THE ARRAYS EACH TIME THE
* OUTPUT INTERVAL IS REACHED.

```

20 DWS=(IS**2.0)*RS*DT
   DRS=(1.0E10*SWFREQ*DT)
   DI1=((RS*(I2+DI2/2.0)-(RC+RS)*(I1+DI1/2.0))*DT)+
>(LS*DI2))/(LC+LS)
   DI2=((RS*(I1+DI1/2.0)-(KS+RL)*(I2+DI2/2.0))*DT)+
>(LS*DI1))/(LS+LL)

   I1=I1+DI1
   I2=I2+DI2
   IS=I1-I2
   WS=WS+DWS
   T=T+DT
   RS=RS+DRS
   LV=(I2*RL)+(LL*DI2/DT)
   COUNT=COUNT+1.0

   IF(COUNT.EQ.OUTINT) THEN
     T=T*1E9
     IS=IS/1E3
     LV=LV/1E6
     IND=IND+1

     IF(NOPLT.EQ.3.0) THEN
       TP1(IND)=T
       ISP1(IND)=IS
       LVP1(IND)=LV
       IF(TP1(IND).GE.TP1(IND-1)) TPMAX=TP1(IND)
       IND1=IND
     END IF

     IF(NOPLT.EQ.2.0) THEN
       TP2(IND)=T
       ISP2(IND)=IS
       LVP2(IND)=LV
       IND2=IND
     END IF

     IF(NOPLT.EQ.1.0) THEN
       TP3(IND)=T
       ISP3(IND)=IS
       LVP3(IND)=LV
       IF(LVP3(IND).GE.LVP3(IND-1)) LVPMAX=LVP3(IND)*1.1
       IND3=IND
     END IF

     T=T/1E9
     IS=IS*1E3
     LV=LV*1E6
     COUNT=0.0
     PRINT 3000,T,RS,IS,I2,LV,WS

```

END IF

IF(IS.GT.ISF) GO TO 20

NOPLT=NOPLT-1.0

IF(NOPLT.GT.0.0) GO TO 10

- * PRINT THE NUMBER OF ARRAY LOCATION USED
- * FOR EACH PLOT TO DETERMINE IF YOU HAVE
- * EXCEEDED THE ALLOTTED NUMBER OF MEMORY
- * LOCATIONS (MAXIMUM OF 60 LOCATIONS).

PRINT 4000,IND1,IND2,IND3
4000 FORMAT(3(5X,I5))

TPINC=TPMAX/4.0

ISPINC=ISPMAX/4.0

LVPINC=LVPMAX/4.0

- * CALL THE DISSPLA PLOTTING ROUTINE TO PLOT
- * SWITCH CURRENT VS TIME AND SWITCH VOLTAGE
- * VS TIME.

CALL COMPRS

CALL BGNPL(+1)

CALL HEIGHT(.2)

CALL TITLE(' ', -1, 'TIME (NSEC)',
>11, 'SWITCH CURRENT (KAMPS)', 22, 8., 6.)
CALL GRAF(0., TPINC, TPMAX, 0., ISPINC, ISPMAX)
CALL CURVE(TP1, ISP1, IND1, 0)
CALL CURVE(TP2, ISP2, IND2, 0)
CALL CURVE(TP3, ISP3, IND3, 0)
CALL ENDPL(0)

CALL TITLE(' ', -1, 'TIME (NSEC)',
>11, 'SWITCH VOLTAGE (MVOLTS)', 23, 8., 6.)
CALL GRAF(0., TPINC, TPMAX, 0., LVPINC, LVPMAX)
CALL CURVE(TP1, LVP1, IND1, 0)
CALL CURVE(TP2, LVP2, IND2, 0)
CALL CURVE(TP3, LVP3, IND3, 0)

CALL DONEPL(0)

END

RUN,F=SWITCH,FTN5
 ENTER THE CURRENT LEVEL IN AMPS:
 63300 CM STORAGE USED.
 0.284 CP SECONDS COMPILATION TIME. 1000
 ENTER THE SWITCHING FREQUENCY IN HERTZ: 10
 ENTER THE LOAD INDUCTANCE IN HENRIES: .7E-6
 ENTER THE OUTPUT INTERVAL: 245

T	RS	IS	I2	LV	WS
0.	0.	.1000E+4	0.	0.	0.
.2450E-9	.2450E+2	.9979E+3	.2131E+1	.1217E+5	.2983E-2
.4900E-9	.4900E+2	.9915E+3	.8515E+1	.2423E+5	.1188E-1
.7350E-9	.7350E+2	.9809E+3	.1907E+2	.3598E+5	.2646E-1
.9800E-9	.9800E+2	.9663E+3	.3366E+2	.4727E+5	.4637E-1
.1225E-8	.1225E+3	.9478E+3	.5210E+2	.5797E+5	.7110E-1
.1470E-8	.1470E+3	.9257E+3	.7417E+2	.6795E+5	.1001E+0
.1715E-8	.1715E+3	.9003E+3	.9959E+2	.7711E+5	.1326E+0
.1960E-8	.1960E+3	.8718E+3	.1280E+3	.8534E+5	.1679E+0
.2205E-8	.2205E+3	.8406E+3	.1592E+3	.9257E+5	.2053E+0
.2450E-8	.2450E+3	.8070E+3	.1927E+3	.9876E+5	.2440E+0
.2695E-8	.2695E+3	.7715E+3	.2282E+3	.1039E+6	.2832E+0
.2940E-8	.2940E+3	.7343E+3	.2653E+3	.1078E+6	.3224E+0
.3185E-8	.3185E+3	.6960E+3	.3036E+3	.1107E+6	.3607E+0
.3430E-8	.3430E+3	.6568E+3	.3427E+3	.1126E+6	.3978E+0
.3675E-8	.3675E+3	.6172E+3	.3822E+3	.1133E+6	.4331E+0
.3920E-8	.3920E+3	.5775E+3	.4219E+3	.1131E+6	.4663E+0
.4165E-8	.4165E+3	.5380E+3	.4613E+3	.1120E+6	.4971E+0
.4410E-8	.4410E+3	.4991E+3	.5002E+3	.1100E+6	.5253E+0
.4655E-8	.4655E+3	.4611E+3	.5382E+3	.1072E+6	.5509E+0
.4900E-8	.4900E+3	.4241E+3	.5751E+3	.1038E+6	.5739E+0
.5145E-8	.5145E+3	.3884E+3	.6108E+3	.9984E+5	.5941E+0
.5390E-8	.5390E+3	.3541E+3	.6450E+3	.9538E+5	.6119E+0
.5635E-8	.5635E+3	.3216E+3	.6775E+3	.9055E+5	.6273E+0
.5880E-8	.5880E+3	.2907E+3	.7083E+3	.8543E+5	.6405E+0
.6125E-8	.6125E+3	.2617E+3	.7372E+3	.8011E+5	.6518E+0
.6370E-8	.6370E+3	.2346E+3	.7643E+3	.7468E+5	.6612E+0
.6615E-8	.6615E+3	.2094E+3	.7895E+3	.6923E+5	.6690E+0
.6860E-8	.6860E+3	.1861E+3	.8128E+3	.6380E+5	.6755E+0
.7105E-8	.7105E+3	.1647E+3	.8342E+3	.5848E+5	.6807E+0
.7350E-8	.7350E+3	.1451E+3	.8537E+3	.5331E+5	.6850E+0
.7595E-8	.7595E+3	.1273E+3	.8715E+3	.4833E+5	.6884E+0
.7840E-8	.7840E+3	.1112E+3	.8875E+3	.4359E+5	.6911E+0
.8085E-8	.8085E+3	.9675E+2	.9020E+3	.3910E+5	.6932E+0
.8330E-8	.8330E+3	.8380E+2	.9149E+3	.3490E+5	.6948E+0
.8575E-8	.8575E+3	.7228E+2	.9264E+3	.3099E+5	.6961E+0
.8820E-8	.8820E+3	.6207E+2	.9366E+3	.2737E+5	.6970E+0
.9065E-8	.9065E+3	.5308E+2	.9456E+3	.2406E+5	.6977E+0
.9310E-8	.9310E+3	.4519E+2	.9535E+3	.2104E+5	.6983E+0
.9555E-8	.9555E+3	.3832E+2	.9603E+3	.1831E+5	.6987E+0

.9800E-8	.9800E+3	.3235E+2	.9663E+3	.1586E+5	.6990E+0
.1004E-7	.1004E+4	.2719E+2	.9714E+3	.1366E+5	.6992E+0
.1029E-7	.1029E+4	.2276E+2	.9759E+3	.1172E+5	.6993E+0
.1053E-7	.1053E+4	.1897E+2	.9797E+3	.1000E+5	.6995E+0
.1078E-7	.1078E+4	.1575E+2	.9829E+3	.8497E+4	.6995E+0
.1102E-7	.1102E+4	.1301E+2	.9856E+3	.7184E+4	.6996E+0
.1127E-7	.1127E+4	.1071E+2	.9879E+3	.6046E+4	.6996E+0
.1151E-7	.1151E+4	.8778E+1	.9898E+3	.5065E+4	.6997E+0
.1176E-7	.1176E+4	.7164E+1	.9914E+3	.4224E+4	.6997E+0
.1200E-7	.1200E+4	.5822E+1	.9928E+3	.3507E+4	.6997E+0
.1225E-7	.1225E+4	.4712E+1	.9939E+3	.2899E+4	.6997E+0
.1249E-7	.1249E+4	.3799E+1	.9948E+3	.2386E+4	.6997E+0
.1274E-7	.1274E+4	.3050E+1	.9956E+3	.1955E+4	.6997E+0
.1298E-7	.1298E+4	.2439E+1	.9962E+3	.1596E+4	.6997E+0
.1323E-7	.1323E+4	.1943E+1	.9967E+3	.1298E+4	.6997E+0
.1347E-7	.1347E+4	.1542E+1	.9971E+3	.1052E+4	.6997E+0
.1372E-7	.1372E+4	.1219E+1	.9974E+3	.8498E+3	.6997E+0

ENTER THE CURRENT LEVEL IN AMPS: 1000

ENTER THE SWITCHING FREQUENCY IN HERTZ: 50

ENTER THE LOAD INDUCTANCE IN HENRIES: .7E-6

ENTER THE OUTPUT INTERVAL: 110

T	RS	IS	I2	LV	WS
0.	0.	.1000E+4	0.	0.	0.
.1100E-9	.5500E+2	.9979E+3	.2137E+1	.2717E+5	.2991E-2
.2200E-9	.1100E+3	.9914E+3	.8561E+1	.5424E+5	.1194E-1
.3300E-9	.1650E+3	.9808E+3	.1919E+2	.8062E+5	.2662E-1
.4400E-9	.2200E+3	.9661E+3	.3388E+2	.1060E+6	.4667E-1
.5500E-9	.2750E+3	.9475E+3	.5245E+2	.1300E+6	.7157E-1
.6600E-9	.3300E+3	.9252E+3	.7467E+2	.1523E+6	.1007E+0
.7700E-9	.3850E+3	.8996E+3	.1003E+3	.1729E+6	.1334E+0
.8800E-9	.4400E+3	.8709E+3	.1289E+3	.1913E+6	.1690E+0
.9900E-9	.4950E+3	.8395E+3	.1603E+3	.2075E+6	.2066E+0
.1100E-8	.5500E+3	.8057E+3	.1940E+3	.2213E+6	.2455E+0
.1210E-8	.6050E+3	.7700E+3	.2297E+3	.2326E+6	.2849E+0
.1320E-8	.6600E+3	.7326E+3	.2670E+3	.2415E+6	.3242E+0
.1430E-8	.7150E+3	.6941E+3	.3055E+3	.2479E+6	.3626E+0
.1540E-8	.7700E+3	.6547E+3	.3448E+3	.2518E+6	.3998E+0
.1650E-8	.8250E+3	.6150E+3	.3845E+3	.2534E+6	.4351E+0
.1760E-8	.8800E+3	.5751E+3	.4243E+3	.2528E+6	.4683E+0
.1870E-8	.9350E+3	.5355E+3	.4638E+3	.2501E+6	.4991E+0
.1980E-8	.9900E+3	.4965E+3	.5028E+3	.2456E+6	.5273E+0
.2090E-8	.1045E+4	.4583E+3	.5409E+3	.2393E+6	.5528E+0
.2200E-8	.1100E+4	.4213E+3	.5779E+3	.2315E+6	.5756E+0
.2310E-8	.1155E+4	.3855E+3	.6136E+3	.2225E+6	.5958E+0
.2420E-8	.1210E+4	.3513E+3	.6478E+3	.2124E+6	.6135E+0
.2530E-8	.1265E+4	.3188E+3	.6803E+3	.2015E+6	.6287E+0
.2640E-8	.1320E+4	.2880E+3	.7110E+3	.1899E+6	.6418E+0
.2750E-8	.1375E+4	.2590E+3	.7399E+3	.1780E+6	.6529E+0

.2860E-8	.1430E+4	.2320E+3	.7669E+3	.1658E+6	.6622E+0
.2970E-8	.1485E+4	.2069E+3	.7920E+3	.1535E+6	.6699E+0
.3080E-8	.1540E+4	.1837E+3	.8152E+3	.1414E+6	.6763E+0
.3190E-8	.1595E+4	.1624E+3	.8364E+3	.1295E+6	.6814E+0
.3300E-8	.1650E+4	.1429E+3	.8559E+3	.1179E+6	.6856E+0
.3410E-8	.1705E+4	.1253E+3	.8735E+3	.1068E+6	.6889E+0
.3520E-8	.1760E+4	.1093E+3	.8894E+3	.9619E+5	.6915E+0
.3630E-8	.1815E+4	.9500E+2	.9037E+3	.8620E+5	.6936E+0
.3740E-8	.1870E+4	.8219E+2	.9165E+3	.7684E+5	.6952E+0
.3850E-8	.1925E+4	.7080E+2	.9279E+3	.6814E+5	.6964E+0
.3960E-8	.1980E+4	.6073E+2	.9380E+3	.6012E+5	.6973E+0
.4070E-8	.2035E+4	.5186E+2	.9468E+3	.5277E+5	.6980E+0
.4180E-8	.2090E+4	.4410E+2	.9546E+3	.4609E+5	.6985E+0
.4290E-8	.2145E+4	.3734E+2	.9613E+3	.4006E+5	.6989E+0
.4400E-8	.2200E+4	.3148E+2	.9672E+3	.3464E+5	.6992E+0
.4510E-8	.2255E+4	.2643E+2	.9722E+3	.2980E+5	.6994E+0
.4620E-8	.2310E+4	.2209E+2	.9765E+3	.2552E+5	.6996E+0
.4730E-8	.2365E+4	.1838E+2	.9802E+3	.2175E+5	.6997E+0
.4840E-8	.2420E+4	.1523E+2	.9834E+3	.1844E+5	.6997E+0
.4950E-8	.2475E+4	.1257E+2	.9861E+3	.1556E+5	.6998E+0
.5060E-8	.2530E+4	.1032E+2	.9883E+3	.1307E+5	.6998E+0
.5170E-8	.2585E+4	.8446E+1	.9902E+3	.1093E+5	.6998E+0
.5280E-8	.2640E+4	.6880E+1	.9917E+3	.9095E+4	.6999E+0
.5390E-8	.2695E+4	.5580E+1	.9930E+3	.7533E+4	.6999E+0
.5500E-8	.2750E+4	.4507E+1	.9941E+3	.6211E+4	.6999E+0
.5610E-8	.2805E+4	.3624E+1	.9950E+3	.5097E+4	.6999E+0
.5720E-8	.2860E+4	.2903E+1	.9957E+3	.4165E+4	.6999E+0
.5830E-8	.2915E+4	.2315E+1	.9963E+3	.3388E+4	.6999E+0
.5940E-8	.2970E+4	.1839E+1	.9968E+3	.2745E+4	.6999E+0
.6050E-8	.3025E+4	.1455E+1	.9971E+3	.2214E+4	.6999E+0
.6160E-8	.3080E+4	.1146E+1	.9975E+3	.1779E+4	.6999E+0

ENTER THE CURRENT LEVEL IN AMPS: 1000
 ENTER THE SWITCHING FREQUENCY IN HERTZ: 100
 ENTER THE LOAD INDUCTANCE IN HENRIES: .7E-6
 ENTER THE OUTPUT INTERVAL: 80

T	RS	IS	I2	LV	WS
0.	0.	.1000E+4	0.	0.	0.
*****	.8000E+2	.9977E+3	.2253E+1	.3938E+5	.3153E-2
.1600E-9	.1600E+3	.9909E+3	.9038E+1	.7873E+5	.1261E-1
.2400E-9	.2400E+3	.9797E+3	.2026E+2	.1170E+6	.2810E-1
.3200E-9	.3200E+3	.9642E+3	.3577E+2	.1537E+6	.4923E-1
.4000E-9	.4000E+3	.9446E+3	.5537E+2	.1893E+6	.7543E-1
.4800E-9	.4800E+3	.9211E+3	.7878E+2	.2205E+6	.1060E+0
.5600E-9	.5600E+3	.8942E+3	.1057E+3	.2498E+6	.1403E+0
.6400E-9	.6400E+3	.8640E+3	.1358E+3	.2759E+6	.1774E+0
.7200E-9	.7200E+3	.8311E+3	.1687E+3	.2986E+6	.2164E+0
.8000E-9	.8000E+3	.7958E+3	.2039E+3	.3178E+6	.2566E+0
.8800E-9	.8800E+3	.7585E+3	.2412E+3	.3332E+6	.2972E+0

.9600E-9	.9600E+3	.7196E+3	.2800E+3	.3449E+6	.3374E+0
.1040E-8	.1040E+4	.6796E+3	.3199E+3	.3530E+6	.3766E+0
.1120E-8	.1120E+4	.6390E+3	.3605E+3	.3574E+6	.4141E+0
.1200E-8	.1200E+4	.5980E+3	.4015E+3	.3584E+6	.4496E+0
.1280E-8	.1280E+4	.5571E+3	.4423E+3	.3562E+6	.4827E+0
.1360E-8	.1360E+4	.5166E+3	.4828E+3	.3509E+6	.5131E+0
.1440E-8	.1440E+4	.4768E+3	.5224E+3	.3430E+6	.5408E+0
.1520E-8	.1520E+4	.4382E+3	.5611E+3	.3327E+6	.5656E+0
.1600E-8	.1600E+4	.4008E+3	.5984E+3	.3204E+6	.5875E+0
.1680E-8	.1680E+4	.3649E+3	.6342E+3	.3063E+6	.6068E+0
.1760E-8	.1760E+4	.3307E+3	.6683E+3	.2909E+6	.6234E+0
.1840E-8	.1840E+4	.2984E+3	.7006E+3	.2744E+6	.6377E+0
.1920E-8	.1920E+4	.2680E+3	.7310E+3	.2571E+6	.6497E+0
.2000E-8	.2000E+4	.2396E+3	.7593E+3	.2395E+6	.6598E+0
.2080E-8	.2080E+4	.2132E+3	.7857E+3	.2217E+6	.6682E+0
.2160E-8	.2160E+4	.1889E+3	.8100E+3	.2039E+6	.6750E+0
.2240E-8	.2240E+4	.1666E+3	.8323E+3	.1865E+6	.6806E+0
.2320E-8	.2320E+4	.1462E+3	.8526E+3	.1696E+6	.6851E+0
.2400E-8	.2400E+4	.1278E+3	.8710E+3	.1533E+6	.6886E+0
.2480E-8	.2480E+4	.1111E+3	.8876E+3	.1378E+6	.6914E+0
.2560E-8	.2560E+4	.9621E+2	.9025E+3	.1231E+6	.6936E+0
.2640E-8	.2640E+4	.8292E+2	.9158E+3	.1095E+6	.6952E+0
.2720E-8	.2720E+4	.7115E+2	.9276E+3	.9676E+5	.6965E+0
.2800E-8	.2800E+4	.6076E+2	.9379E+3	.8507E+5	.6975E+0
.2880E-8	.2880E+4	.5166E+2	.9470E+3	.7440E+5	.6982E+0
.2960E-8	.2960E+4	.4371E+2	.9549E+3	.6471E+5	.6987E+0
.3040E-8	.3040E+4	.3683E+2	.9618E+3	.5599E+5	.6991E+0
.3120E-8	.3120E+4	.3088E+2	.9678E+3	.4819E+5	.6994E+0
.3200E-8	.3200E+4	.2578E+2	.9729E+3	.4126E+5	.6996E+0
.3280E-8	.3280E+4	.2142E+2	.9772E+3	.3515E+5	.6997E+0
.3360E-8	.3360E+4	.1772E+2	.9809E+3	.2979E+5	.6998E+0
.3440E-8	.3440E+4	.1459E+2	.9840E+3	.2511E+5	.6999E+0
.3520E-8	.3520E+4	.1196E+2	.9867E+3	.2107E+5	.6999E+0
.3600E-8	.3600E+4	.9758E+1	.9889E+3	.1758E+5	.7000E+0
.3680E-8	.3680E+4	.7926E+1	.9907E+3	.1460E+5	.7000E+0
.3760E-8	.3760E+4	.6409E+1	.9922E+3	.1207E+5	.7000E+0
.3840E-8	.3840E+4	.5159E+1	.9935E+3	.9922E+4	.7000E+0
.3920E-8	.3920E+4	.4134E+1	.9945E+3	.8119E+4	.7000E+0
.4000E-8	.4000E+4	.3297E+1	.9953E+3	.6611E+4	.7000E+0
.4080E-8	.4080E+4	.2619E+1	.9960E+3	.5358E+4	.7000E+0
.4160E-8	.4160E+4	.2070E+1	.9965E+3	.4322E+4	.7000E+0
.4240E-8	.4240E+4	.1630E+1	.9970E+3	.3471E+4	.7000E+0
.4320E-8	.4320E+4	.1277E+1	.9973E+3	.2774E+4	.7000E+0
.4400E-8	.4400E+4	.9969E+0	.9976E+3	.2208E+4	.7000E+0
57	57	56			

PLOTTING COMMENCING

.....

VITA

James M. Gruden was born on May 27, 1958 in Washington, Pennsylvania. He graduated as the cosalutatorian of his high school class in Houston, Pennsylvania in 1976. He entered the United States Air Force on October 28, 1976. After basic training at Lackland AFB and an eight-month technical school at Lowry AFB, he was assigned to the Air Force Flight Dynamics Laboratory at Wright-Patterson AFB as an instrumentation mechanic. Having received a scholarship through the Airman Scholarship and Commissioning Program, he then attended the University of Pittsburgh to work on his Bachelor of Science degree in Electrical Engineering. He graduated cum laude in May 1982 and received his commission in the United States Air Force through the ROTC program.. He entered the School of Engineering, Air Force Institute of Technology, in June 1982.

Permanent Address:

192 Ellington Road
Dayton, OH 45431

UNCLASSIFIED

SECURITY CLASSIFICATION OF THIS PAGE

REPORT DOCUMENTATION PAGE

1a. REPORT SECURITY CLASSIFICATION UNCLASSIFIED			1b. RESTRICTIVE MARKINGS		
2a. SECURITY CLASSIFICATION AUTHORITY			3. DISTRIBUTION/AVAILABILITY OF REPORT Approved for public release; distribution unlimited.		
2b. DECLASSIFICATION/DOWNGRADING SCHEDULE					
4. PERFORMING ORGANIZATION REPORT NUMBER(S) AFIT/GE/EE/83D-22			5. MONITORING ORGANIZATION REPORT NUMBER(S)		
6a. NAME OF PERFORMING ORGANIZATION School of Engineering		6b. OFFICE SYMBOL (If applicable) AFIT/ENG		7a. NAME OF MONITORING ORGANIZATION	
6c. ADDRESS (City, State and ZIP Code) Air Force Institute of Technology Wright-Patterson AFB, Ohio 45433				7b. ADDRESS (City, State and ZIP Code)	
8a. NAME OF FUNDING/SPONSORING ORGANIZATION Aero Propulsion Laboratory		8b. OFFICE SYMBOL (If applicable) POOS-2		9. PROCUREMENT INSTRUMENT IDENTIFICATION NUMBER	
8c. ADDRESS (City, State and ZIP Code) Wright-Patterson AFB, Ohio 45433				10. SOURCE OF FUNDING NOS.	
				PROGRAM ELEMENT NO.	PROJECT NO.
11. TITLE (Include Security Classification) See Box 19					
12. PERSONAL AUTHOR(S) James M. Gruden, Second Lieutenant, USAF					
13a. TYPE OF REPORT MS Thesis		13b. TIME COVERED FROM _____ TO _____		14. DATE OF REPORT (Yr., Mo., Day) 1983 December	
15. PAGE COUNT 89					
16. SUPPLEMENTARY NOTATION <div style="text-align: right;">Approved for public release: 1AW AFB 190-17. <i>John E. WOLAVER</i> 7 Feb 84 Dean for Research and Professional Development Air Force Institute of Technology Wright-Patterson AFB OH 45433</div>					
17. COSATI CODES			18. SUBJECT TERMS (Continue on reverse if necessary and identify by block number) Electrical Switches, Electric Contacts, Electrical Brushes		
FIELD 09	GROUP 01	SUB GR			
19. ABSTRACT (Continue on reverse if necessary and identify by block number) Title: REPETITIVE SWITCHING FOR AN ELECTROMAGNETIC RAIL GUN Thesis Advisor: Timothy L. Skvarenina, Major, USAF					
20. DISTRIBUTION/AVAILABILITY OF ABSTRACT UNCLASSIFIED/UNLIMITED <input checked="" type="checkbox"/> SAME AS RPT. <input type="checkbox"/> DTIC USERS <input type="checkbox"/>				21. ABSTRACT SECURITY CLASSIFICATION UNCLASSIFIED	
22a. NAME OF RESPONSIBLE INDIVIDUAL Timothy L. Skvarenina, Major, USAF				22b. TELEPHONE NUMBER (Include Area Code) 513-255-6913	
				22c. OFFICE SYMBOL AFIT/ENG	

DD FORM 1473, 83 APR

EDITION OF 1 JAN 73 IS OBSOLETE.

UNCLASSIFIED

SECURITY CLASSIFICATION OF THIS PAGE

This study investigates several modifications of a repetitive opening switch. The switch design consists of a rotating copper disk (rotor) with a pie-shaped insulator section and brushes which slide along the rotor surface. The modifications include two new brush designs and the placement of tungsten inserts at the copper-insulator interfaces of the rotor.

One brush design (fringe fiber) employs carbon fibers on the leading and trailing edge of the brush to increase the resistive commutating action as the switch opens and closes. The other brush design uses "fingers" to conduct current to the rotor surface, effectively increasing the number of brush contact points. The rotor modification was the placement of tungsten inserts at the copper-insulator interfaces. It was hoped that the increased resistivity and hardness of the tungsten inserts would reduce the arcing between the brushes and the rotor surface and lessen the arc related damage of the switch.

The new rotor design was very successful. The arc related damage at the insulator section interface was reduced by the tungsten inserts and a larger resistive commutating action was observed due to its presence. The fringe fiber brush design did not work well at the high current levels where the switch was designed to operate. In fact, many of the fibers were completely detached from the brush at current levels above 4 kA. The finger brushes also had difficulty conducting current above the 4 kA level. During these runs, the fingers began to melt and in some cases the brushes became unsoldered from the brush straps.

END

FILMED

4-84